Journal of Structural Geology, Vol. 14, No. 6, pp. 723 to 742, 1992
Printed in Great Britain

0191-8141/92 $05.00+0.00

Progressive deformation in anisotropic rocks

RUUD WEIJERMARS*

Hans Ramberg Tectonic Laboratory, Department of Mineralogy and Petrology, Institute of Geology, Uppsala University, Box 555, S-751 22 Uppsala, Sweden

(*Received* 17 *June* 1991; *accepted in revised form* 27 *January* 1992)

Abstract—Field observations show that the majority of crustal rocks possess a penetrative foliation defined by either compositional layering, preferred orientations of crystals, or both. Ductile deformation involving planar anisotropy of viscosity can be characterized by an anisotropy factor $\delta = \eta_N/\eta_S$, the ratio of the bulk viscosities in pure and simple shear, respectively. This ratio of the normal and shear viscosities may be determined analytically if the anisotropy is resolvable in a multilayer sequence with individual laminae of isotropic viscosity. In that case, the resistance to normal compression will be largely controlled by the competent layers, whereas the resistance to shear is controlled by the soft layers. More specifically, the viscosities of the individual laminae add up like resistances in series and in parallel in the expressions for the normal and shear viscosities, respectively.

The reorientation of the bulk stress within an anisotropic multilayer is systematically investigated for a range of anisotropy factors. The mode of progressive deformation is controlled only by the anisotropy factor and the orientation of the principal deviatoric stress. The rate of deformation can be scaled if the bulk normal viscosity and the magnitude of the principal deviatoric stress are also known. The results are illustrated in a series of nomograms showing the spectrum of strain and rotation histories possible in rock volumes deforming with planar anisotropy. It appears that with increasing anisotropy factor the deformation spectrum will narrow on simple shear, irrespective of the orientation of the background or bulk deviatoric stress axes. Plane strain and isochoric conditions are assumed throughout the analysis.

INTRODUCTION

IT IS usually assumed that rock is isotropic in its mechanical response to a stress field at depths, allowing ductile flow by solid-state crystalloplastic creep. This assumption of isotropic flow keeps the analytical description simple, since the principal axes of strain-rate or incremental strain remain parallel to those of stress. It is then possible to predict from the viscosity and the orientation of the stress field which finite deformation may occur after a particular time, by integrating the velocity gradient equations. This procedure has been rationalized in a companion paper (Weijermars 1991), advancing previous studies on ductile, progressive deformation in isotropic rock (Ramberg 1975a,b, Pfiffner & Ramsay 1982).

The limitation of this approach is that it is only applicable to isotropic rocks, whereas many natural rocks are mechanically anisotropic. For example, field observations show that most crustal rocks possess a penetrative foliation defined by either compositional layering, preferred orientation of crystals, or both. Modelling of the mantle suggests that, there also, compositional layering may be maintained by stretching subducted heterogeneities into thin layers alternating with primordial mantle rocks of different composition (Allègre & Turcotte 1986) or development of preferred crystallographic orientation (Christensen 1987, Nicolas 1989, Ribe 1989).

Previous investigations, discussed below, have shown that the constitutive relationship between stress and strain-rate in anisotropic rocks is different from that in isotropic rocks. This is because the viscosity—a scalar in isotropic media—becomes a tensor quantity in anisotropic flow in order to account for the directional variation in the magnitude of the viscosity. Principal axes of stress no longer need to remain parallel to those of incremental strain or strain-rate. For example, deformation by progressive simple shear in isotropic rocks is maintained by a bulk stress with the major principal stress and strain-rate axes both oriented at 45° to the direction of shear. It is demonstrated here that in strongly anisotropic rocks the bulk stress may be oriented at almost any angle to the direction of anisotropy—deformation will consistently occur by progressive simple shear parallel to the direction of the anisotropy. Stress trajectories inside anisotropic rocks may deviate from the orientation of the principal axes of bulk stress (see later).

The tensor approach also yields a relationship between the bulk stress and bulk strain-rate (magnitude and orientation of principal axes) in terms of the viscosities and thicknesses of the individual laminae of any viscous multilayer. The present paper adopts the anisotropy factor delta (δ), introduced by Honda (1986), and expands its application to quantify how finite strain develops in a ductile medium for various degrees of anisotropy and arbitrary orientations of the bulk deviatoric stress. This relationship has not been elaborated in any previous study.

PREVIOUS WORK AND PRESENT SCOPE

Past research on the role of mechanical anisotropy in ductile regimes has been fragmentary. Nonetheless, two

* Present address: Earth Science Department, King Fahd University of Petroleum and Minerals, 312 61 Dhahran, Saudi Arabia.

major schools can be distinguished: geophysical and geological. The similarity between the analytical descriptions of viscous and elastic deformation (cf. Biot 1965) has been employed by both schools to transfer equations governing anisotropic elasticity to viscous flow in anisotropic media. Most earlier work is restricted to stratified media comprising thin planar layers of internally isotropic viscosity, so that the symmetry axis of the anisotropy of the multilayer itself is oriented perpendicular to the layering. The planar anisotropy is aligned with the convective streamlines in numerical models of mantle flow (Christensen 1987) and chevron folded in semi-numerical models of similar folding (Casey & Huggenberger 1985, Ridley & Casey 1989). In elastic literature this particular type of planar anisotropy has been termed "orthotropic" (Jaeger & Cook 1979) or "transversely isotropic" (Banik 1987).

The theory of Backus (1962) concerning anisotropic elasticity has been adopted in preliminary attempts to model anisotropic flow in the Earth's mantle (Saito & Abe 1984, Honda 1986). The adapted *geophysical* theory applies to multilayers comprising thin parallel layers of ductile rock with different Newtonian viscosity separated by plane and coherent interfaces of no-slip. The aim of these studies is to find how the anisotropy affects the convective streamline pattern in the mantle. No inference was made about the relationship between principal axes of stress and strain-rate. The degree of anisotropy was characterized by a non-dimensional number δ. However, the nature of the anisotropy was limited to multilayers comprising repetitions of two different rheological components only and assumptions were made about the relative thickness and minimum viscosity contrast of the layers.

Biot's (for references see Biot 1961, 1965) theories concerning buckling of orthotropic elastic multilayers have been transformed to multilayers with orthotropic viscosity profiles in the *geological* literature (Cobbold *et al.* 1971, Cobbold 1976, Johnson 1977, Cobbold & Watkinson 1981, Latham 1985). Research focused on the refraction of stress and strain across rheological interfaces within such multilayers (Bayly 1970, Strömgård 1973, Treagus 1973, 1981, 1983, 1985, 1988). Two valuable expressions have been derived for predicting the refraction of the principal stress axis orientation (Strömgård 1973, Treagus 1973) and the magnitude of the shear strain component either side of a rheological interface (Cobbold 1983, Treagus 1983). These expressions are rederived here (see Appendix, equations A23 and A28) and complemented with several other equations of practical importance.

Previous inferences about the mode of *progressive deformation* in orthotropic rocks were limited because (1) the degree of anisotropy was not quantified and (2) the viscosity was not formulated as a tensor quantity. The concept of a viscosity tensor has been outlined in work on anisotropic mantle flow (Honda 1986) and may be elaborated and applied to geological realms where development of finite deformation patterns is of interest. The rheological effects of anisotropy can be best characterized and quantified by the anisotropy factor δ. In many geological situations, the anisotropy may be in the form of a laminated, compositional multilayer, and how to determine the anisotropy factor for such multilayers is derived here. The velocity gradient equations for anisotropic flow are then integrated and used to illustrate how the degree of anisotropy affects the mode of progressive deformation.

BASIC ASSUMPTIONS

Materials with anisotropic viscosity have an internal structure such that the effective viscosity is different for different modes of deformation. A simple geometry for such anisotropy occurs if the rheology is controlled by either a planar compositional layering or a penetrative foliation due to preferred orientation of crystal fabrics. In the following derivation of a constitutive flow law for orthotropic anisotropy, consider a laminated medium comprising several parallel layers $a(=1, \ldots, q)$ of infinite lateral extent and internally isotropic viscosity. The multilayer has its plane of anisotropy perpendicular to the X-axis of a Cartesian co-ordinate system XYZ (Fig. 1). The deformation is due to biaxial incompressible flow in the XZ-plane which causes plane strain only. Consequently, the major and minor principal axes of all stress and strain-rate ellipsoids lie within the XZ-plane. Assume that the anisotropy remains planar, that no slip occurs along the interfaces, interfacial tension is absent, the fluids are incompressible and fluid interfaces remain coherent throughout the deformation.

The total state of stress at any point is described by three principal stress axes $\sigma_1 \geq \sigma_2 \geq \sigma_3$. It is important to distinguish clearly between total and deviatoric stress. Principal axes of total and deviatoric stress will remain parallel in both isotropic and anisotropic media. However, the magnitude of the terms in the deviatoric part of the stress tensor S_{ij} (whether bulk or local) are related by the tensor expression:

$$T_{ij} = S_{ij} + P_{ij}, \tag{1}$$

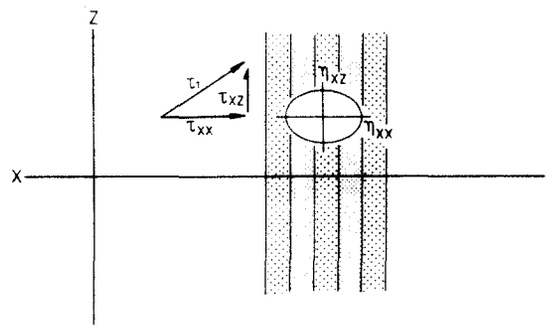

Fig. 1. Multilayer oriented with the layers of anisotropic viscosity parallel to the YZ-plane. The normal and shear components η_{xx} and η_{xz} of the viscosity tensor η_{ij} are graphically represented by the ellipse. The ellipsoid representation is just an arbitrary visual tool to show the anisotropy orientation. The shear viscosity η_{xz} should not be confused with the normal viscosity η_{zz}, which has the same orientation, but different magnitude (i.e. $\eta_{zz} = \eta_{xx}$).

with deviatoric stress tensor T_{ij} and hydrostatic stress tensor $P_{ij} = -P\delta_{ij} = -1/3\sigma_{kk}\delta_{ij}$, taking $\delta_{ij} = 1$ for $i = j$ and $\delta_{ij} = 0$ for $i \neq j$. The boundary condition of plane strain requires that $\sigma_2 = P$ which implies $\sigma_2 = (1/2)(\sigma_1 + \sigma_3)$, so that:

$$\tau_1 = \sigma_1 - \sigma_2 = (1/2)(\sigma_1 - \sigma_3) \tag{2a}$$

$$\tau_2 = 0 \tag{2b}$$

$$\tau_3 = \sigma_3 - \sigma_2 = (1/2)(\sigma_3 - \sigma_1). \tag{2c}$$

This assumes that the deformation is incompressible, and therefore the deviatoric stress $\tau_1 = -\tau_3$. The adjective 'bulk' will be applied to denote quantities valid for the flow at length scales larger than the characteristic spacing of the laminae in the multilayer; i.e. those quantities directly related to forces exerted at the outer surface of the rock volume studied. The principal axes of stress and strain rate within any of the individual layers $a(=1, \ldots, q)$ of the multilayer will all remain within the XZ-plane.

To simplify the discussion, only deviatoric stresses will be considered in what follows unless stated otherwise. Assume that no deviatoric stresses other than those caused by the principal surface stress exist in the multilayer, i.e. stresses due to primary and thermally induced density variations are excluded. The magnitudes of the normal and shear components of the deviatoric stress tensor cannot be constructed as vector quantities, but may be calculated from the two principal deviatoric stresses within the plane of flow using Mohr's equations (see Appendix). If the deformation is truly planar and remains in the XZ-plane, the bulk deviatoric stress tensor T_{ij} and strain rate tensor D_{ij} are:

$$T_{ij} = \begin{bmatrix} \tau_{xx} & 0 & \tau_{xz} \\ 0 & 0 & 0 \\ \tau_{xz} & 0 & -\tau_{xx} \end{bmatrix} \tag{3}$$

$$D_{ij} = \begin{bmatrix} \dot{e}_{xx} & 0 & \dot{e}_{xz} \\ 0 & 0 & 0 \\ \dot{e}_{xz} & 0 & -\dot{e}_{xx} \end{bmatrix}. \tag{4}$$

The only two independent components of the bulk deviatoric stress tensor and the strain-rate tensor are mutually related by the normal and shear component of the viscosity tensor η_{ij} in:

$$\begin{bmatrix} \tau_{xx} \\ \tau_{xz} \end{bmatrix} = \begin{bmatrix} 2\eta_{xx} & 0 \\ 0 & 2\eta_{xz} \end{bmatrix} \begin{bmatrix} \dot{e}_{xx} \\ \dot{e}_{xz} \end{bmatrix}. \tag{5}$$

The bulk effective viscosity of a body with orthotropic anisotropy will vary with the orientation of the stress field applied, and therefore becomes a tensor quantity itself. The diagonal and two-suffix form of the viscosity tensor in expression (5) results from the choice of the YZ-plane parallel to the planes of anisotropy. Solutions for the viscosity tensor components in a multilayer with stepped rheology profiles will be derived below. The results will then be generalized for any orthotropic anisotropy and arbitrary orientations of the co-ordinate axes.

Normal viscosity

The relationship between the τ_{xx}-component of the bulk stress tensor, the bulk pure-shear strain-rate $\dot{e}_{xx}$ and the η_{xx}-component of the bulk viscosity tensor is (cf. equation 5):

$$\eta_{xx} = \tau_{xx}/2\dot{e}_{xx}. \tag{6}$$

Extrusion of any soft layers is inhibited due to infinite lateral extent of the multilayer and the no-slip condition at the interface with the adjoining layers (Fig. 2). Consequently, the normal strain-rates $\dot{e}_{xx(a)}$ (for $a = 1, \ldots, q$) within individual laminae of thickness d_a in the multilayer, must have a particular constant value equal to the bulk shear strain-rate $\dot{e}_{xx}$:

$$\dot{e}_{xx} = \dot{e}_{xx(1)} = \dot{e}_{xx(2)} = \cdots = \dot{e}_{xx(q)}. \tag{7}$$

The normal component σ_{zz} $(=-\sigma_{xx})$ of the total bulk stress is the mean of the stresses $\sigma_{zz(a)}$ in each of the individual layers of thickness d_a in the multilayer divided by total thickness d:

$$\sigma_{zz} = (1/d)\sum_{a=1}^{q}(d_a\sigma_{zz(a)})$$

$$= (1/d)\sum_{a=1}^{q}(-P_a + 2\eta_a\dot{e}_{zz})d_a \tag{8a}$$

or

$$\sigma_{zz} = (-1/d)\sum_{a=1}^{q}(P_a + 2\eta_a\dot{e}_{xx})d_a. \tag{8b}$$

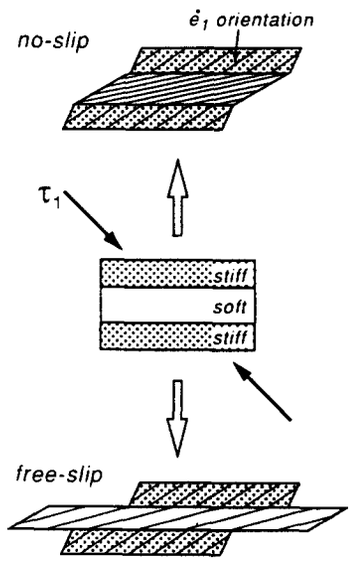

Fig. 2. Deformation of a simplified anisotropic multilayer by an oblique principal stress τ_1. The normal component of strain-rate in the soft and stiff layers may not remain equal if slip along the interfaces is possible, so that the soft layer will extrude (bottom). However, the normal strains and strain-rates *will* be equal in all layers if their interfaces have to remain coherent and rigid due to no-slip boundary conditions (top). The shear component of the strain-rate will always be different in the stiff and soft layers, i.e. higher in the soft layers, independent of the boundary conditions. Adapted from an illustration originally used for a different purpose by Suppe (1985, fig. 10-10).

The boundary condition at each interface is that the total normal stress $\sigma_{xx} = \sigma_{xx(a)} = \sigma_{xx(b)}$, so that:

$$-P + \tau_{xx} = -P_a + \tau_{xx(a)} = -P_b + \tau_{xx(b)}. \quad (9)$$

The pressure will be different in layers of different viscosity, so that $P_a \neq P_b$.

Using expressions (6) and (8a) together with (9) to eliminate P_a yields:

$$\eta_{xx} = (1/2)\left[(d_a/d)\frac{\tau_{xx(a)}}{\dot{e}_{xx(a)}} + \cdots + (d_q/d)\frac{\tau_{xx(q)}}{\dot{e}_{xx(q)}}\right]$$

$$= \sum_{a=1}^{q} (\eta_a d_a^*) \quad (10)$$

with normalized thickness $d_a^* = d_a/d$. The viscosities η_a (for $a = 1, \ldots, q$) of the individual layers in the multilayer add up as in a series configuration of resistances in the expression for the bulk normal viscosity η_{xx}. This means that the resistance to normal compression (without any extrusion of the softer layers) will be largely controlled by the stiffer layers (higher effective viscosity, higher resistance) of the multilayer.

Shear viscosity

The relationship between the τ_{xz}-component of the bulk deviatoric stress tensor, the bulk simple-shear strain-rate $\dot{e}_{xz}$ and the η_{xz}-component of the bulk viscosity tensor is (cf. equation 5):

$$\eta_{xz} = \tau_{xz}/2\dot{e}_{xz} = \tau_{xz}/\gamma \quad (11)$$

with tensor strain-rate $\dot{e}_{xz}$ and engineering strain-rate γ related by $\dot{e}_{xz} = \gamma/2$. If one outer surface is fixed the bulk engineering strain-rate γ is related to the velocity (v_z) of the other outer surface of the multilayer by:

$$\gamma = v_z/d. \quad (12)$$

The outer surface velocity itself is the sum of the velocities in the individual laminae of the multilayer, which may all have different magnitudes:

$$v_z = \sum_{a=1}^{q} d_a(\partial v_z/\partial x)_a = \sum_{a=1}^{q} (d_a\gamma_a). \quad (13)$$

The boundary condition of no-slip at the interface implies that the shear stress $\tau_{xz(a)}$ (for $a = 1, \ldots, q$) is equal to the bulk shear stress τ_{xz} applied to drive the shear component of the flow:

$$\tau_{xz} = \tau_{xz(1)} = \tau_{xz(2)} = \cdots = \tau_{xz(q)}. \quad (14)$$

Insertion of equations (12)–(14) into (11) yields:

$$\eta_{xz} = (\tau_{xz}d)/v_z = \frac{\tau_{xz}}{(d_a/d)\gamma_a + \cdots + (d_q/d)\gamma_q}$$

$$= \frac{1}{d_a^*\frac{\gamma_a}{\tau_{xz(a)}} + \cdots + d_q^*\frac{\gamma_q}{\tau_{xz(q)}}}$$

$$= 1\Big/\sum_{a=1}^{q} (d_a^*/\eta_a). \quad (15)$$

The viscosities η_a (for a = 1, ..., q) of the individual layers in the multilayer add up in the same fashion as parallel resistances in the expression for the bulk shear viscosity η_{xz}. This means that the resistance to simple shearing will be predominantly controlled by the softer layers (low effective viscosity, low resistance) in the multilayer.

FLOW IN MULTILAYER WITH ANISOTROPIC RHEOLOGY AND ARBITRARY ORIENTATION IN CARTESIAN SPACE

So far, the normal components of the bulk stress, viscosity and strain-rate tensors, τ_{kk}, η_{kk} and $\dot{e}_{kk}$, respectively, have all remained parallel to each other due to the particular orientation of the reference frame in Fig. 1. If the plane of anisotropy has an arbitrary orientation with respect to the co-ordinate axes, the direction of normal stresses will not generally coincide with that of normal viscosities. The principal directions of the viscosity anisotropy are those connected to coaxial flow, either perpendicular or parallel to the plane of layering, both denoted by η_N, and the shear parallel to the layering is controlled by η_S.

Assume that the plane of anisotropy has an arbitrary orientation in XYZ-space. The viscosity anisotropy can then be expressed in a fourth-order tensor $\eta_{ij\,kl}$ which relates the second-order tensors T_{ij} and D_{kl} in a generalized constitutive equation:

$$T_{ij} = 2\eta_{ij\,kl}D_{kl}. \quad (16)$$

In a general three-dimensional flow, equation (16) represents nine separate equations, containing 81 viscosity constants in total (cf. Nye 1957, p. 133), e.g.:

$$\tau_{11} = 2(\eta_{11\,11}\dot{e}_{11} + \eta_{11\,12}\dot{e}_{12} + \eta_{11\,13}\dot{e}_{13} + \eta_{11\,21}\dot{e}_{21} + \eta_{11\,22}\dot{e}_{22} + \eta_{11\,23}\dot{e}_{23} + \eta_{11\,31}\dot{e}_{31} + \eta_{11\,32}\dot{e}_{32} + \eta_{11\,33}\dot{e}_{33}). \quad (17)$$

For the two-dimensional incompressible flow considered here, it is convenient to keep the Y-axis parallel to the plane of anisotropy and perpendicular to the plane of strain (Fig. 3). In this case there are only three independent components of η_{ijkl} and the components of the stress and strain-rate tensors in the XZ-system are related by the expression:

$$\begin{bmatrix}\tau_{xx}\\ \tau_{xz}\end{bmatrix} = \begin{bmatrix}2\eta_{xx\,xx} & 2\eta_{xx\,xz}\\ 2\eta_{xz\,xx} & 2\eta_{xz\,xz}\end{bmatrix}\begin{bmatrix}\dot{e}_{xx}\\ \dot{e}_{xz}\end{bmatrix}. \quad (18)$$

The viscosity tensor is symmetric ($\eta_{ij\,kl} = \eta_{kl\,ij}$) so that $\eta_{xx\,xz} = \eta_{xz\,xx}$. The viscosity tensor components of the principal viscosities η_N and η_S with respect to the XZ-coordinates can be obtained using the transformation rules for fourth-rank tensors. If the X-axis is defined at an arbitrary angle ϕ with respect to the normal or pole to

the plane of anisotropy (Fig. 3) the viscosity components are:

$$\eta_{xx\,xx} = \eta_N \cos^2 2\phi + \eta_S \sin^2 2\phi \quad (19)$$

$$\eta_{xz\,xz} = \eta_N \sin^2 2\phi + \eta_S \cos^2 2\phi \quad (20)$$

$$\eta_{xx\,xz} = (\eta_N - \eta_S) \cos 2\phi \sin 2\phi. \quad (21)$$

See also Cobbold (1976). Recall now that:

$$\eta_N = \sum_{a=1}^{q} (\eta_a d_a^*) \quad \text{(cf. equation 10)} \quad (22)$$

$$\eta_S = 1 \Big/ \sum_{a=1}^{q} (d_a^*/\eta_a) \quad \text{(cf. equation 15).} \quad (23)$$

The ratio (η_N/η_S) of the normal and shear viscosities has been termed the anisotropy factor δ (Honda 1986, p. 1455, equation 8b):

$$\delta = \eta_N/\eta_S. \quad (24)$$

This ratio of viscosity under shear and normal stress is sufficient to model anisotropic flow numerically. However, for construction of anisotropic model analogues composed of internally isotropic multilayers, it is necessary to apply the formulation as developed in the previous section. It will be shown in the next section that the anisotropy factor δ has a specific physical meaning in the sense that it is a direct measure of the difference in orientation of the principal axes of bulk stress and bulk strain-rate.

INCLINATION OF BULK STRESS AND STRAIN-RATE AXES IN ANISOTROPIC MULTILAYERS

The axes of principal stress and principal strain-rate remain parallel throughout the deformation history of flows of isotropic fluids. This is not the general case in the deformation of anisotropic multilayers. Within individual isotropic layers of such multilayers, stress and strain-rate axes remain parallel, but *this is not generally true for the principal axes of the bulk stress and bulk strain-rate ellipsoids* (cf. Fig. A1). An expression derived below relates the angles between the principal axes of the strain-rate and stress ellipsoids of the bulk deformation. Additionally, expressions are derived for calculating the magnitudes of the principal stresses and strain-rates within each of the individual laminae of the multilayer, provided that the external stress field and viscosity parameters are known (see Appendix). The refraction or change in orientation of the principal stress and strain-rate axes across the interface between adjacent layers is an intrinsic property controlled by the viscosity ratio alone (see Appendix). Most equations derived are also applicable to deformation of rocks where the anisotropy is due to a mineral fabric of otherwise homogeneous composition.

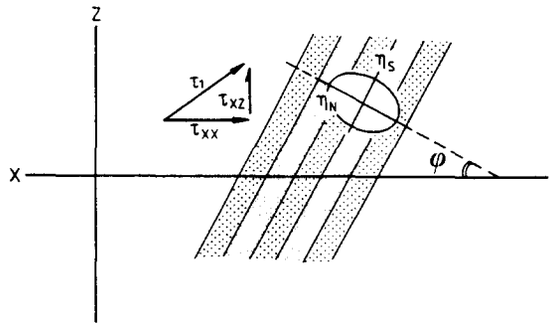

Fig. 3. Anisotropic multilayer inclined to the X-axis but parallel to the Y-axis. The normal and shear components of the viscosity are denoted by η_N and η_S, respectively. The angle ϕ is referred to in the co-ordinate transformation equations (19)–(21).

Consider a multilayer which has its plane of anisotropy perpendicular to the X-axis (cf. Fig. 1). All of the deformation is within the XZ-plane and is governed by a plane strain-rate ellipsoid with the intermediate axis parallel to the Y-axis so that $\dot{e}_1 = -\dot{e}_3$. The angle ξ between the bulk principal stress axis τ_1 and the pole to the plane of anisotropy (Fig. 4) can be expressed as (using $\tau_{xx} = \tau_1 \cos 2\xi$ and $\tau_{xx} = \tau_1 \sin 2\xi$, see Appendix):

$$\cot 2\xi = \tau_{xx}/\tau_{xz}. \quad (25)$$

Substitution of expression (25) into (A26) yields:

$$\xi_a = (1/2) \tan^{-1} [(\tan 2\xi)(\eta_N/\eta_a)]. \quad (26)$$

The angle ψ between the bulk principal strain-rate axis $\dot{e}_1$ and the plane of anisotropy (Fig. 4) can be expressed as (from the ratio of equations A9 and A10):

$$\cot 2\psi = \dot{e}_{xx}/\dot{e}_{xz}. \quad (27)$$

Substitution of expression (27) into (A32) gives:

$$\psi_a = (1/2) \tan^{-1} [(\tan 2\psi)(\eta_S/\eta_a)]. \quad (28)$$

The angles ψ_a and ξ_a are measured from reference lines 90° apart to take into account the fact that the largest stretch of the incremental strain ellipsoid, S_1, is perpendicular to τ_1. Expressions (26) and (28) can therefore

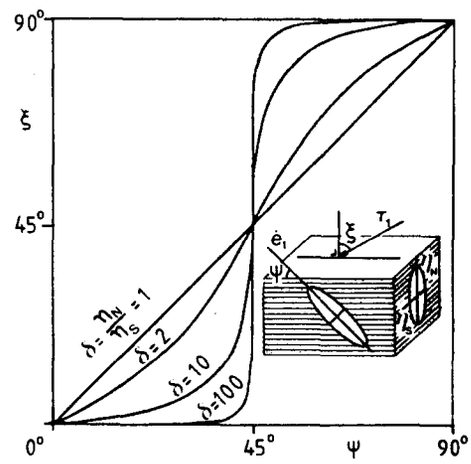

Fig. 4. Plot illustrating the physical meaning of the anisotropy factor $\delta = \eta_N/\eta_S$. (After Cobbold 1976, fig. 5.) If the material is isotropic ($\delta = 1$), then the axes of the stress and strain-rate ellipsoids will be inclined at similar angles (ξ and ψ, respectively) with respect to any plane boundary, so that their principal axes will coincide. However, if the material is anisotropic with viscosity components η_N and η_S (so that $\delta > 1$), then ξ and ψ will generally be different.

be equated because $\xi_a = \psi_a$ in isotropic layers $a = 1, \ldots, q$, so that:

$$\tan 2\psi/\tan 2\xi = \eta_N/\eta_S. \quad (29)$$

Expression (29) demonstrates that the anisotropy factor $\delta = \eta_N/\eta_S$ can be used as a direct measure for the difference between the orientations of the bulk principal stress and strain-rate axes with respect to the plane of anisotropy. Figure 4 illustrates this physical meaning of δ by plotting the orientation of the principal axes of the bulk stress and bulk strain-rate (see also Cobbold 1976, fig. 5). It appears that their respective axes coincide if τ_1 is parallel, perpendicular or inclined at 45° to the plane of anisotropy. However, if the anisotropy factor is large ($\delta > 100$), the axes of the bulk strain-rate for the multilayer will generally remain consistently inclined at approximately 45° to the layering or anisotropy plane, irrespective of the orientation of the bulk stress axes, so long as the latter are not parallel or perpendicular to the layering.

This quantitative result can be qualitatively understood in the following fashion. A strain-rate ellipsoid oriented at 45° to the bedding of the multilayer corresponds to the case of plane simple shear, which—in isotropic materials—occurs only if τ_1 is inclined at exactly 45° with respect to the planes of motion. However, the presence of *a strong anisotropy* (i.e. $\delta > 100$) apparently *inhibits the multilayer deforming in any other fashion than by simple shear*, unless two axes of the stress coincide with the plane of anisotropy. More specifically, an approximate progressive simple shear will always occur if the anisotropy factor $\delta > 100$ for any $0° < \xi < 90°$. In constant strain-rate experiments with $\dot{e}_1$ oblique to the layering, the orientation ξ of τ_1 may wobble anywhere between 0° and 90° if $\delta > 100$ (Fig. 4). If the anisotropy is defined by a multilayer comprising laminae of finite thicknesses and internally isotropic viscosities, the magnitudes of η_N and η_S are given by expressions (22) and (23), respectively.

DESCRIPTION AND VISUALIZATION OF PROGRESSIVE DEFORMATION

Deformation occurring uninterrupted with time is termed progressive and implies a continuous sequence of configurations through which a body passes, unlike the general term 'deformation' which refers to the difference in geometry of two distinct finite states of a body (Flinn 1962). Progressive deformation paths in isotropic rocks have been studied systematically (Ramberg 1975a,b, 1986, Pfiffner & Ramsay 1982, Weijermars 1991), but systematic study of progressive deformation in anisotropic rocks has not previously been attempted. The mathematical framework provided here makes it possible to quantify progressive deformation in terms of the anisotropy factor and orientation of the bulk principal stress axis.

Consider a block of material of anisotropic viscosity resting on a stable plane, termed the reference plane in what follows (Fig. 5). The reference plane coincides with the XY-surface and deformation occurs in the XZ-plane. Deformation is isochoric and homogeneous on the scale studied, which implies that the anisotropy is penetrative and uniform within the block. The mathematical descriptions providing the framework to track progressive deformation have been discussed in detail elsewhere (Weijermars 1991). The movement path of any particle (x_o, y_o, z_o) is described by the deformation tensor expression:

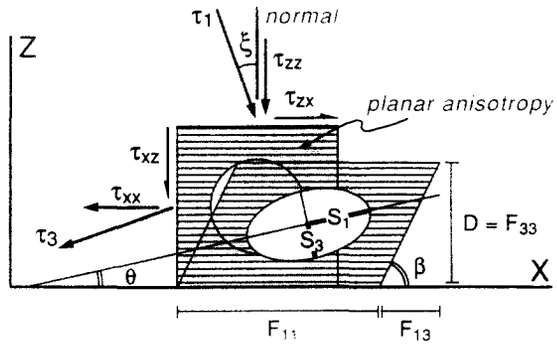

Fig. 5. Definition diagram showing a section through the deforming unit volume and the angle ξ of the principal deviatoric stress τ_1 with respect to the normal to the reference plane. The anisotropy is parallel to the XY-plane and its intensity may be varied using scaling parameter δ. The inclination θ of the major axis of the strain ellipsoid, and its principal stretch S_1 are used to quantify progressive deformation in Figs. 6 and 7(a)–(d). The inclination β of the cube's side and its orthogonal height D are used to quantify progressive deformation in the absence of other strain markers as portrayed in Figs. 8 and 9(a)–(d). The tensor elements F_{11}, F_{13} and F_{33} relate to physical lengths as indicated.

$$(x, y, z) = \mathbf{F}(x_o, y_o, z_o) \quad (30)$$

with $\mathbf{F}$ the deformation tensor and (x_o, y_o, z_o) and (x, y, z) the position vectors of an arbitrary material particle before and after deformation. In the case of homogeneous plane strain in the XZ-plane, only four of the nine elements of the deformation tensor are non-zero if the X-axis is chosen parallel to a non-rotating, free-slip boundary to the deforming volume (Fig. 5). This detachment plane may be interpreted as a stretching fault, using a new terminology for faults moving contemporaneously with ductile deformation of the wall rock (Means 1990). The four non-zero tensor elements, F_{11}, F_{13}, F_{22}, F_{33}, may then be expressed in the following dynamic terms (Weijermars 1991):

$$F_{11} = \exp(\dot{e}_{xx}t) \quad (31a)$$

$$F_{13} = (2\dot{e}_{xz}/\dot{e}_{xx}) \sinh(\dot{e}_{xx}t) \quad (31b)$$

$$F_{22} = 1 \quad (31c)$$

$$F_{33} = \exp(-\dot{e}_{xx}t). \quad (31d)$$

Expressions (31a)–(31d) were obtained by time-integrating the rate-of-displacement equations, and can be linked to the stress tensor as follows. The strain-rate components are linked to the stress by expression (18) and need to include the anisotropy factor $\delta = \eta_N/\eta_S$ if applied to anisotropic rocks:

$$\dot{e}_{xx} = \tau_{xx}/2\eta_N \quad (32a)$$

$$\dot{e}_{xz} = \tau_{xz}/2\eta_S = \delta\tau_{xz}/2\eta_N. \quad (32b)$$

The normal and shear strain-rates can now be related directly to the orientation ξ of the principal deviatoric stress τ_1 with respect to the normal of the reference plane (Fig. 3), making use of the equations for the Mohr circle of stress for incompressible, two-dimensional flow ($\tau_{xx} = \tau_1 \cos 2\xi$ and $\tau_{xz} = \tau_1 \sin 2\xi$):

$$\dot{e}_{xx} = (\tau_1 \cos 2\xi)/(2\eta_N) \quad (33a)$$

$$\dot{e}_{xz} = \delta(\tau_1 \sin 2\xi)/(2\eta_N). \quad (33b)$$

The variable matrix elements F_{11}, F_{13}, F_{33} in expressions (31) may now be rewritten by substitution of expressions (35a) and (35b):

$$F_{11} = \exp(R_t \cos 2\xi) \quad (34a)$$

$$F_{13} = (F_{11} - F_{11}^{-1})\delta \tan 2\xi \quad (34b)$$

$$F_{22} = 1 \quad (34c)$$

$$F_{33} = F_{11}^{-1}, \quad (34d)$$

where the only three independent variables are δ, anisotropy, ξ, the angle between the smallest principal deviatoric stress τ_1 and the normal to the reference plane (Fig. 5), and the non-dimensional time $R_t = (t\tau_1)/2\eta_N$. Arbitrary quantities are time t, major principal stress τ_1, and normal viscosity η_N. Positive angles of ξ are measured anti-clockwise from the normal to the reference plane.

Expression (30), using tensor elements of expressions (34a)–(34d), is practical for forward modelling of progressive deformation, using arbitrary stress orientations ξ and normalized times R_t (cf. Weijermars 1991). Figure 5 explains how the matrix elements F_{11}, F_{13} and F_{33} are physically expressed as the normalized dimensions of a model cube deforming along a detachment horizon acting as a reference plane. Two types of passive markers are considered: (a) spheres and (b) cubes (Fig. 5). These will be discussed in turn.

(a) *Spherical markers*

The deformation history of spherical markers, or circles in the plane of strain, may be quantified in terms of the progressive changes in the length of the major stretching axis S_1 of the evolving strain ellipse and the angle θ measured between S_1 and the reference plane (Fig. 5). The stretch S_1 is intrinsic to the deformation tensor and is straightforward if the matrix elements F_{11}, F_{13} and F_{33} are known:

$$S_1 = [0.5(K + [K^2 - 4]^{1/2})]^{1/2} \quad (35a)$$

with $K = F_{11}^2 + F_{13}^2 + F_{33}^2$, provided $F_{31} = 0$. The minor stretching axis S_3 can be determined from the boundary condition of plane isochoric strain so that $S_1S_3 = 1$; the ellipticity or axial ratio is $R = S_1/S_3 = S_1^2$. The angle θ between the finite strain ellipsoid major axis and the X-axis parallel to the reference plane is:

$$\theta = 0.5 \arctan[(2F_{13}F_{33})/(F_{11}^2 + F_{13}^2 - F_{33}^2)]. \quad (35b)$$

The algorithms of expressions (35a) and (35b) were incorporated into a computer program to map the continuous change of both S_1 and θ for any orientation ξ of the bulk principal stress axis with respect to the normal of the plane of anisotropy using various values for the anisotropy factor δ. In order to help explain the profound effect of anisotropy on the character of progressive deformation, it is first shown how S_1 and θ change in *isotropic* rock ($\delta = 1$). Figure 6 graphs the relationship between the inclination angle θ of the strain ellipsoid major axis (with respect to the reference plane) and the magnitude of the major stretch S_1 for a set of values of ξ. In isotropic materials, the axes of the ellipsoids for stress and incremental strain (or strain-rate) coincide so that $\theta = \xi$ at the onset of deformation. They will remain 90° apart, owing to the fact that S_1 of the instantaneous or incremental strain ellipsoid is always perpendicular to τ_1. The subsequent evolution of finite strain and rotation of the strain ellipse is outlined by the nearly horizontal curves in Fig. 6.

The plot of Fig. 6 is non-dimensional, except for the vertical isochrons. They are scaled for the particular case of rock with an isotropic viscosity of 5×10^{21} Pa s deforming by a principal deviatoric stress of 100 MPa, corresponding to a characteristic strain-rate of 10^{-14} s^{-1}. The isochrons are included in Fig. 6 to bring out clearly that pure shear is a mechanism much more effective than simple shear for achieving large strains for a given stress field. This applies only to isotropic rheologies; the reverse holds for orthotropic viscosities where the plane of weakness lies in the shear direction (see below).

Figures 7(a)–(d) are similar to Fig. 6, but show the change of θ and S_1 for progressive deformation in rocks with *anisotropy* factors δ = 2, 3, 5, 10, 25 and 100, respectively. The isochron patterns (using $\eta_N = 5 \times 10^{21}$ Pa s and τ_1 = 100 MPa) show that even for rocks with only weak anisotropy (δ = 2, Fig. 7a) pure shear is no longer more effective than simple shear for achieving large finite deformations. Deformation preferentially occurs by simple shear and accumulates faster for larger anisotropy factors. Even if the principal stress axis is close to orientations characteristic for nearly pure shear (e.g. ξ = 80° or 10°), deformation will tend towards simple shear rather than pure shear if $\delta > 100$ (Fig. 7d). In anisotropic materials, the principal axes of the ellipsoids for stress and incremental strain (or strain-rate) generally do not coincide (so that $\theta \neq \xi$), even at the onset of the deformation.

(b) *Cubic markers*

The deformation history of cubic markers, or squares in the plane of strain, may be quantified in terms of the progressive changes in the orthogonal height of the square and the angle β between the reference plane and an initially vertical marker line of the deforming square (Fig. 5). The height or orthogonal thickness of the square at any time t is equal to $D = F_{33}$ as specified in expression (34d). Any initially vertical line of the cube

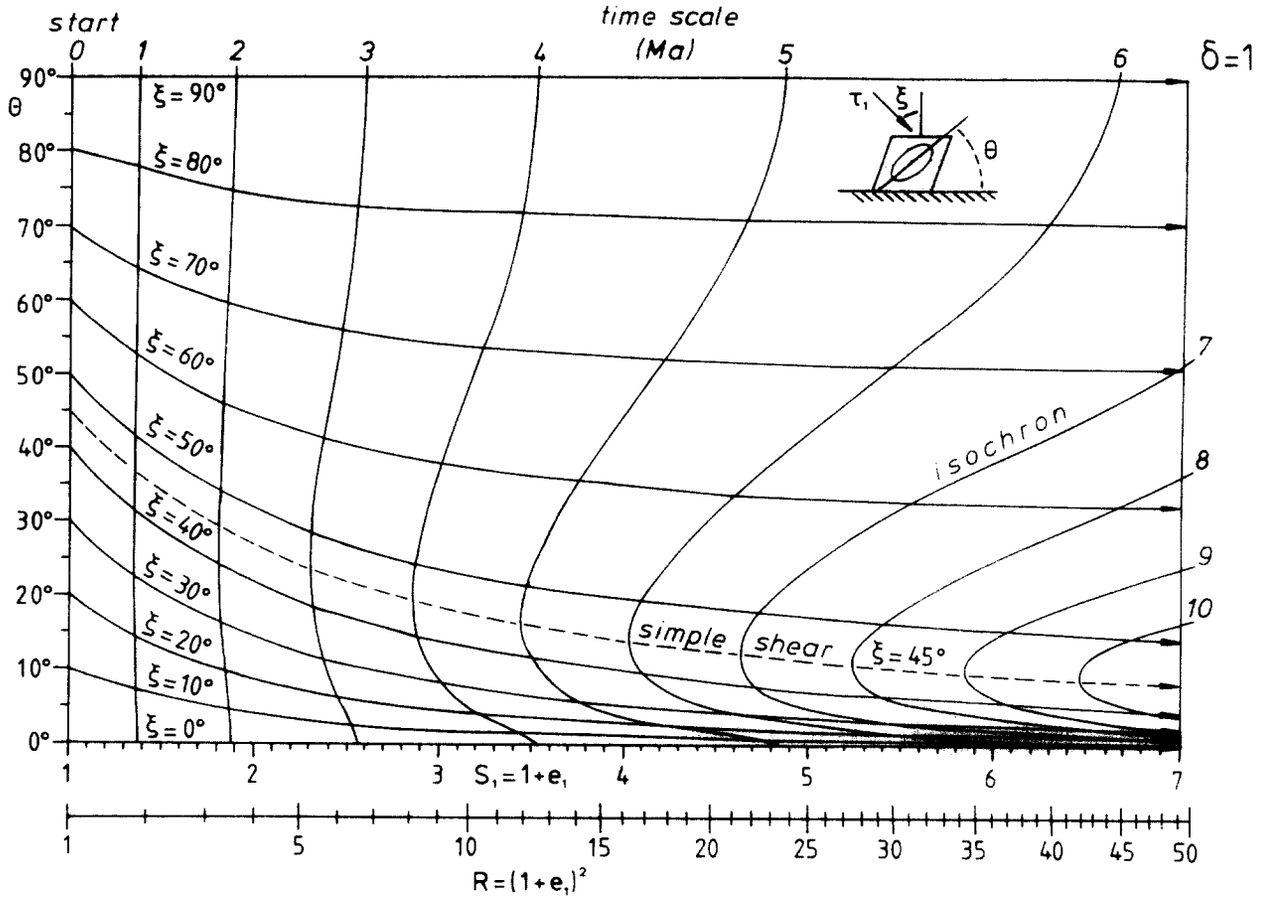

Fig. 6. Nomogram showing parameters characterizing progressive deformation of a passive spherical marker in isotropic rock. Deformation changes the angle θ of the finite strain ellipsoid major axis with respect to a reference plane simultaneously with an increase in the magnitude of the stretch S_1 (or ellipticity R). The specific relationship between θ and S_1 is indicated for deviatoric stresses inclined at 0°, 10°, 20°, 30°, 40°, 45°, 50°, 60°, 70°, 80° and 90° with respect to the reference plane. The isochrons indicate how fast the deformation progresses for the various stress angles, assuming a principal strain-rate of 10^{-14} s^{-1}.

is, after deformation, inclined at an angle β with respect to the reference plane:

$$\beta = \tan^{-1}(F_{11}^{-1}F_{13}^{-1}). \quad (36a)$$

The algorithms of expressions (34d) and (36a) were also incorporated into a computer program to map the continuous change of both D and β for any orientation ξ of the bulk, principal stress axis with respect to the reference plane using various values for the anisotropy factor δ. For completeness, the direct relationship between D and β follows from combining equations (34b) and (36a):

$$\cot\beta = \delta(D^{-1} - 1)\tan 2\xi. \quad (36b)$$

For later comparison with the effect of anisotropy, it is first shown how D and β change in *isotropic* rock ($\delta = 1$) during progressive deformation. Figure 8 is a graph plotting the change in orthogonal thickness D of a deforming layer vs the change in angle β of a marker line initially normal to the layer, for a variety of orientations ξ of the principal stress axis. Layer thickening occurs for $\xi > 45°$ and thinning for $\xi < 45°$, whilst it remains unchanged in simple shear ($\xi = 45°$). Layer thinning is fastest for pure shear at $\xi = 0°$, and fastest thickening occurs by pure shear at $\xi = 90°$. Note that the concave downward 'bulge' in the isochron pattern indicates that the rotation of the cube's side is fastest for simple shear ($\xi = 45°$) at the onset of the deformation. However, a larger total strain accumulates in a given time for smaller values of ξ.

Figures 9(a)–(d) plot parameters similar to those of Fig. 8, but for rock with *anisotropy* factors $\delta = 2, 3, 5$ and 10. It is obvious from comparison with Figs. 8 and 9(d) that for larger values of δ it becomes increasingly difficult to change the height (D) of the initial cube. If δ is sufficiently large ($\delta > 100$), all deformation will occur by simple shear, and initially vertical lines rotate faster away from the vertical for large δ.

GENERALIZATION

The main features concerning the effect of anisotropy on progressive deformation can be thought of in terms of the rate of layer thinning or thickening. Anisotropy affects the shape of particle movement paths and consequently the kinematic vorticity number W_k. This relationship can be quantified as follows. The kinematic vorticity number (Means *et al.* 1980) can be written in terms of the normal and shear strain-rate components of deformation (Bobyarchick 1986, p. 41):

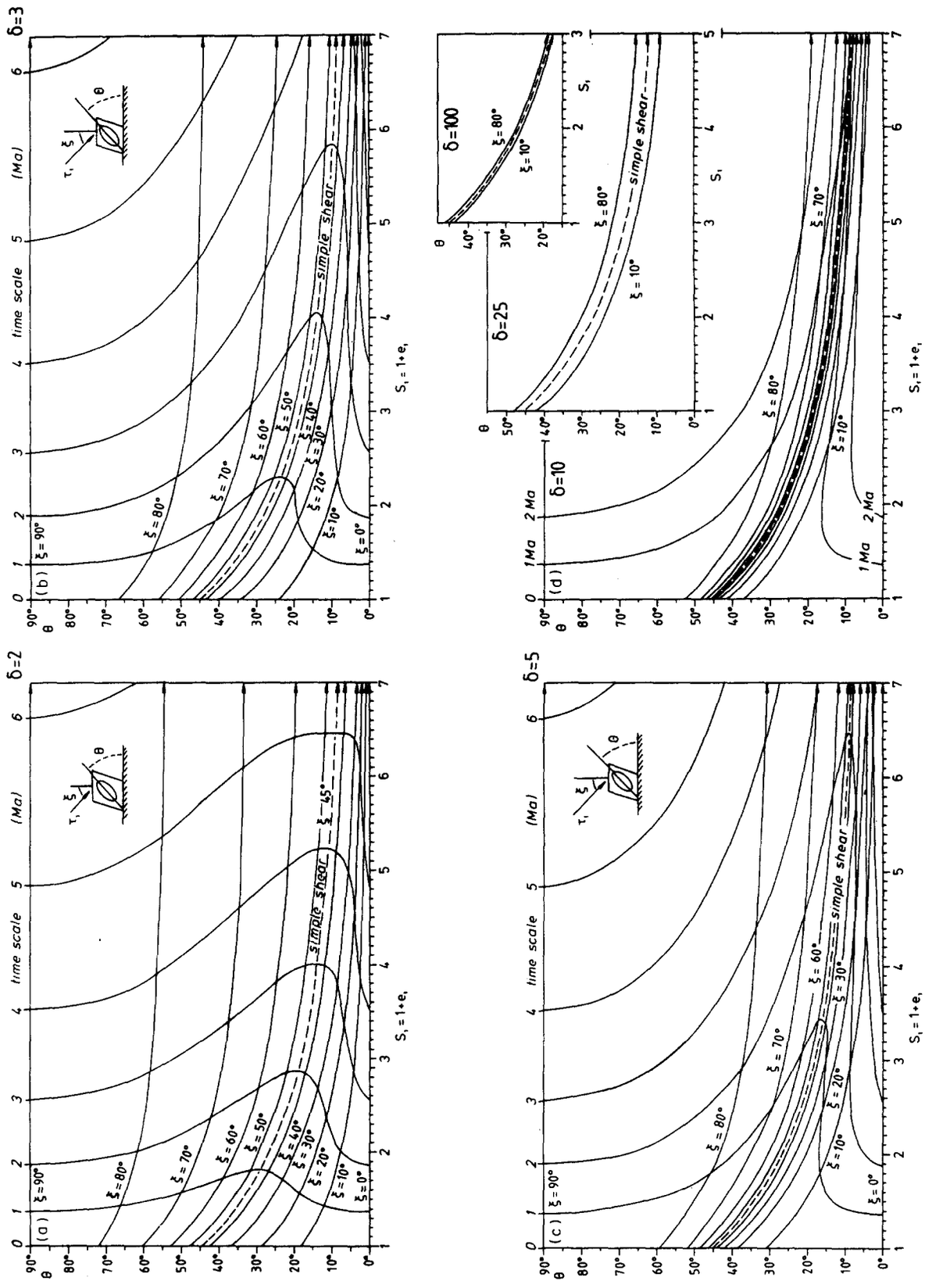

Fig. 7. Nomograms characterizing progressive deformation of a passive spherical marker in rock with anisotropy factor (a) $\delta = 2$, (b) $\delta = 3$, (c) $\delta = 5$ and (d) $\delta = 10$, with insets showing convergence towards simple shear for $\delta = 25$ and $\delta = 100$, keeping η_N constant and diminishing η_S. See text and caption to Fig. 6 for further explanation.

$$W_k = \cos(\tan^{-1}(2\dot{e}/\gamma)). \quad (37a)$$

Since the engineering shear strain-rate γ is related to the tensor shear strain-rate by $2\gamma = \dot{e}_{xz}$, expression (37a) can be rewritten as:

$$W_k = \cos(\tan^{-1}(\dot{e}_{xx}/\dot{e}_{xz})). \quad (37b)$$

Combining expressions (33a) and (33b) yields $\dot{e}_{xx}/\dot{e}_{xz} = \cot 2\xi/\delta$, and substitution into expression (37b) gives an expression relating ξ, the kinematic vorticity number W_k, and the anisotropy factor δ:

$$W_k = \cos(\tan^{-1}((\cot 2\xi)/\delta)). \quad (37c)$$

It follows from expressions (32a) and (32b) that the ratio $\dot{e}_{xx}/\dot{e}_{xz}$ remains constant, assuming a particular orientation of the principal stress axis with respect to the plane of anisotropy, even if the magnitude of τ_1 were varying over time. This complies with the requirement of steady state flow for the application of the kinematic vorticity number.

Figure 10 graphs the relationship between the stress angle ξ and kinematic vorticity number W_k for various values of δ. The orientation ξ of the principal deviatoric stress axis with respect to the normal to the reference plane is plotted along the horizontal axis of Fig. 10. The resulting kinematic vorticity number is plotted along the vertical axis. The curves in (ξ, W_k) space show which kinematic vorticity number arises in response to a particular orientation ξ of τ_1. It illustrates that for $\xi = 45°$, $W_k = 1$ always so that the progressive deformation will be simple shear. For $\xi = 0°$, $W_k = 0$ pure-shear deformation always occurs, leading to layer thinning. $W_k = 0$ also for $\xi = 90°$, but pure shear occurs in a fashion leading to layer thickening. In general, layer thinning occurs if $\xi < 45°$, and thickening occurs for $\xi > 45°$. The kinematic vorticity number can be used as a qualitative measure for the rate at which layer thinning or thickening occurs. It follows from expression (37c) that the kinematic vorticity number varies with δ for any particular orientation $0° < \xi < 45°$ and $45° < \xi < 90°$. W_k is always close to 1 if δ is sufficiently large ($\delta > 100$), provided that $\xi \neq 0°$ or $\xi \neq 90°$.

Figure 10 implies that changes in layer thickness perpendicular to the plane of anisotropy are unlikely to occur if the degree of anisotropy is larger than 100. It also emphasizes that highly anisotropic rocks will deform by approximately simple shear along the plane of anisotropy in almost all cases. W_k is always 0 (pure shear) for any δ provided that $\xi = 0°$ or 90°, but this situation may be unstable, as the slightest deflection of ξ in highly anisotropic rocks would lead to large W_k and approximately simple-shear deformation. This effect may be further illustrated making use of the general stream function, Ψ, for anisotropic flow derived here

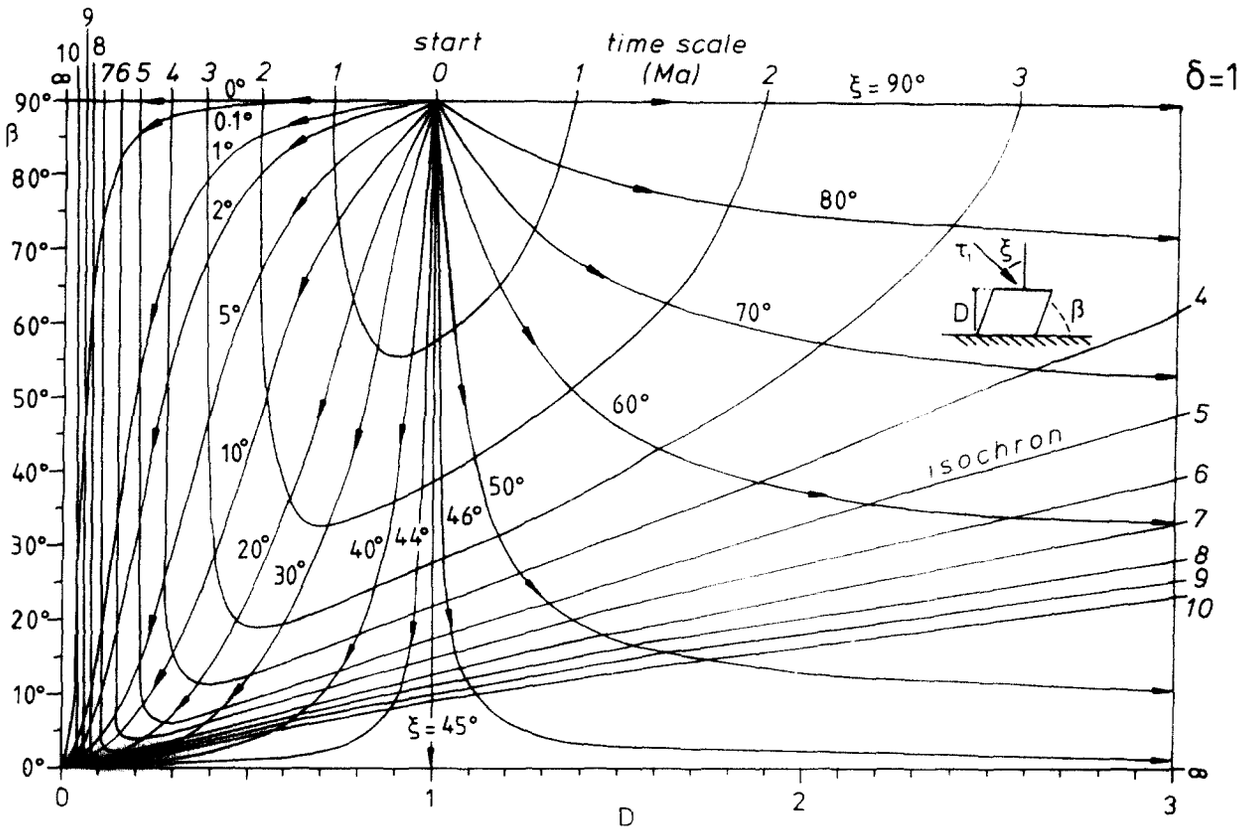

Fig. 8. Nomogram showing parameters characterizing progressive deformation of a passive rectangular marker in isotropic rock. Plotted is the relationship between the change in layer thickness (expressed as stretch D) and the rotation (β) of a line initially orthogonal to the reference plane for various orientations ξ of the deviatoric stress. The angle β is 90° at time 0, when deformation begins. The vertical line $D = 1$ shows that there is no change in layer thickness for simple shear. Note that, in pure-shear deformations, layer thinning or thickening does not involve a change in the angle β, and therefore pure shear plots along the top line of the diagram. See also the definition diagram of Fig. 3.

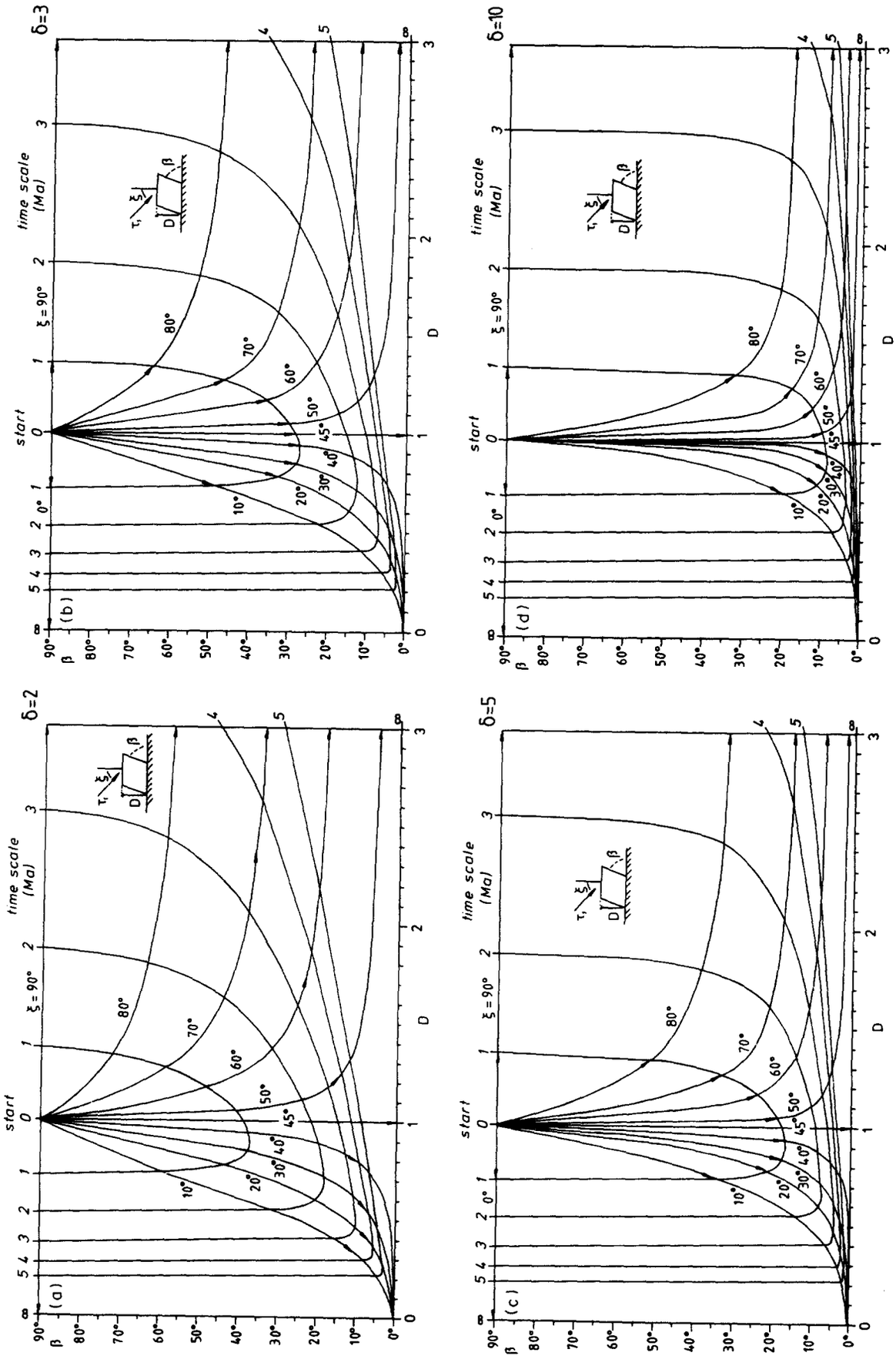

Fig. 9. Nomograms characterizing progressive deformation of a passive rectangular marker in rock with anisotropy factor (a) $\delta = 2$, (b) $\delta = 3$, (c) $\delta = 5$ and (d) $\delta = 10$, keeping η_N constant and diminishing η_S.

without further proof (modified from the general stream function for isotropic flow derived in Weijermars & Poliakov (in preparation):

$$\Psi = B(xz\cos 2\xi + \delta z^2 \sin 2\xi), \qquad (38)$$

with scaling parameter $B = \tau_1/\eta_N$. Figures 11(a)–(d) show how the streamlines or particle movement paths are affected by changing δ and keeping $\xi = 5°$. In isotropic rocks ($\delta = 1$), the streamlines for $\xi = 5°$ approximate those of pure shear (Fig. 11a), but the same stress orientation in anisotropic rocks of $\delta = 30$ causes a flow pattern approximating that of a simple shear (Fig. 11d).

The most complete documentation of the effect of anisotropy makes use of the flow asymptotes (solutions of $\Psi = 0$). These are two straight lines, of which one coincides with the plane of anisotropy and the other makes an angle α (making use of $W_k = \cos\alpha$ and equation 37c):

$$\alpha = \tan^{-1}((\cot 2\xi)/\delta). \qquad (39)$$

Positive angles are measured clockwise from the plane of anisotropy, negative angles are measured anti-clockwise. Figure 12 effectively demonstrates that the two flow asymptotes coincide (i.e. $\alpha = 0°$, simple-shear flow) for almost any orientation ξ of τ_1, provided the anisotropy is sufficiently large ($\delta > 100$).

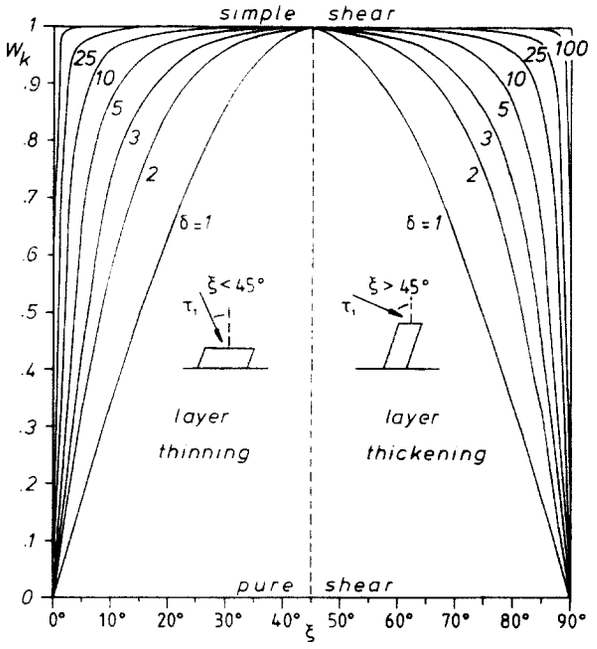

Fig. 10. The relationship between the kinematic vorticity number W_k, anisotropy factor δ, and angle ξ between the major principal stress axis and the normal to the plane of anisotropy, as expressed in equation (37c). The mode of progressive deformation (W_k) is entirely determined by the angle of attack of the external stress field and the intrinsic anisotropy of any particular medium. Deformation is restricted to the plane of view as the deviatoric stress has no component perpendicular to the plane of section. Note how similarly oriented stresses may cause different modes of progressive deformation if the degree of anisotropy is different.

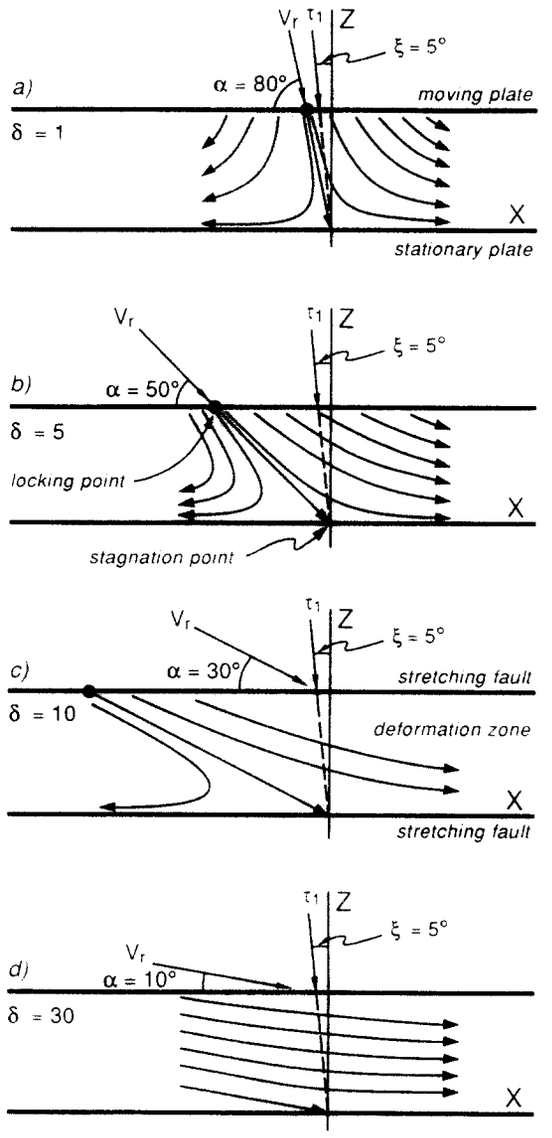

Fig. 11. Flowlines obtained as solutions of the stream function Ψ of equation (38) using a constant stress orientation $\xi = 5°$ for anisotropy (a) $\delta = 1$, (b) $\delta = 5$, (c) $\delta = 10$ and (d) $\delta = 30$. The trace of the plane of anisotropy is parallel to the X-axis, for most convenient solutions of Ψ. The relative velocity vector, V_r, of the upper boundary of the deforming volume is parallel to the flow asymptotes inclined at angle α to the X-axis.

PRACTICAL IMPLICATIONS

Some practical implications of the outlined theory of anisotropic flow are discussed below. The first section shows how variations in the degree of anisotropy may explain lateral variations in the amount of shear along ductile shear zones. The orientation of an anisotropy within a shear zone may determine the occurrence of either transpression or transtension. The next section explains how the intensity and orientation of anisotropy can explain why three different mechanisms of folding may occur. The final section yields practical implications for the formation of grain shape fabrics and hints for laboratory measurements of anisotropy factors.

Shear zones

Shear zones are formed by progressive shear strain localized between two blocks of less strained host rock. It follows from the discussion above that the rheological nature of the rock affected by a shear zone will have a profound effect upon the nature of progressive deformation. Shear zones are layers of localized strain, and therefore these layers must be weaker (i.e. bulk viscosity less) than the host rock. The fact that shear strain profiles across major ductile shear zones typically show an exponential increase in the amount of shear towards the centre of the zones (cf. Simpson 1983, Weijermars & Rondeel 1984, Weijermars 1987a,b), can be explained by profound softening of rocks involved in the shear, either immediately before or during shearing, or both (cf. Fleitout & Froideveaux 1980, Poirier 1980).

We may distinguish two types of shear zones, possessing either rheological stratification or anisotropy coinciding with the orientation of the shear zone (*type* 1, Fig. 13a), or rheological stratification coinciding with the shear zone but with an internal foliation oblique to the direction of shear (*type* 2, Fig. 13c). The classification labels suggested here are entirely arbitrary and unlike previous classifications made on different grounds (cf. Means 1984). The mechanical behaviour of the two types of shear zones can be predicted by the present theory. Whether the width of a ductile shear zone increases, decreases, or remains constant during shear depends on the orientation and intensity of the anisotropy enclosed between the moving walls. This will be explained below.

Type 1. The parts of Fig. 10 with $0° < \xi < 90°$ can be interpreted as illustrating how the rheological stratification of type 1 shear zones reacts to a tectonic stress field of a particular orientation. If the sheared layer is softer than its host rock, but internally still isotropic (i.e. $\delta = 1$), transtension or transpression (cf. Sanderson & Marchini 1984) will occur for any principal stress inclined at angles smaller or larger than 45°, respectively. However, if the rheological stratification defines a strong anisotropy parallel to the shear zone boundaries (i.e. $\delta > 100$), then approximate simple-shear strain will always occur irrespective of the orientation of the principal stress axis (Figs. 13a & b).

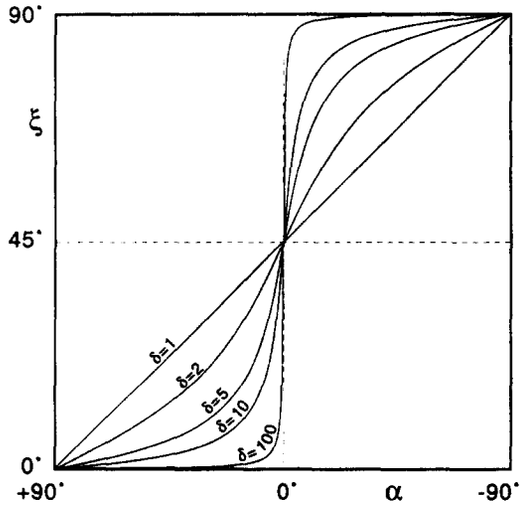

Fig. 12. Plot of flow asymptote orientation, α, with respect to the plane of anisotropy vs stress orientation, ξ, for δ = 1, 2, 5, 10 and 100, according to equation (39).

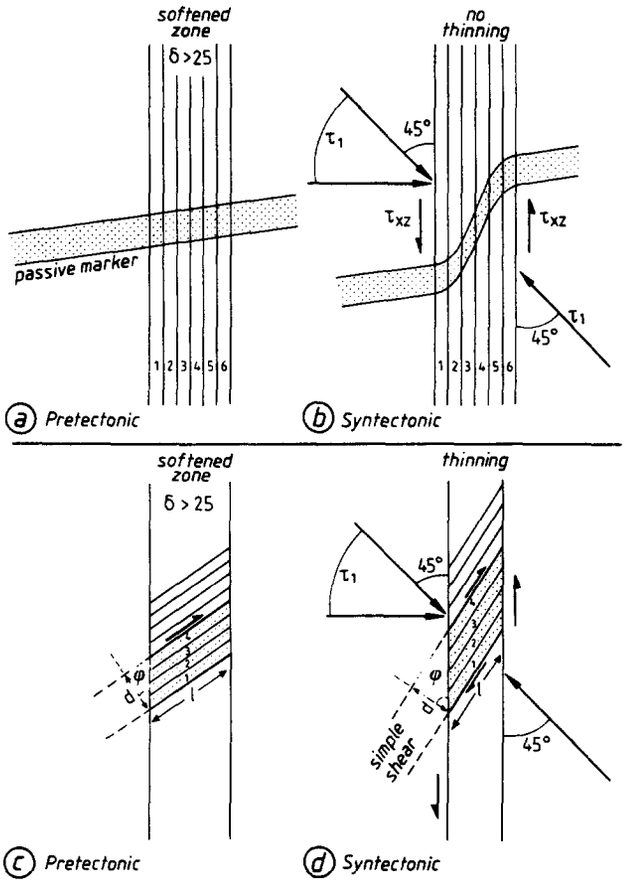

Fig. 13. Whether the width of a ductile shear zone will increase, decrease or remain constant during shear is controlled by the orientation and intensity of anisotropy enclosed between the moving walls. Two shear zones are illustrated, either enclosing strongly anisotropic fabrics, oriented parallel (a & b) and oblique (c & d) to the direction of shear. Progressive shear motion will involve no thinning in the shear zone with wall-parallel anisotropy (a & b). If thinning occurs in the shear zone, the length scales d and L in (c & d) remain constant during the shear motion. Reverse shear motion would involve thickening of the shear zone. The angle ϕ is that used in equations (19)–(21).

Note that variations in the amount of ductile shear strain across and along type 1 shear zones can be explained by variations in the intensity of the anisotropy. This follows from combining expressions (27) and (29), which yields:

$$\dot{e}_{xz} = \dot{e}_{xx}\delta \tan 2\xi. \qquad (40)$$

Expression (40) implies that the shear strain-rate $\dot{e}_{xz}$ in any particular shear zone may vary according to spatial variations in the degree of anisotropy if the magnitude and orientation of the principal stress near the shear zone boundaries remain constant (so that $\dot{e}_{xx}$ wil be space invariant). A lateral increase in the anisotropy factor δ will cause a proportional increase in the strain-rate.

Type 2. Assume a shear zone composed of a softened layer with an internal foliation oblique to the direction of

shear as illustrated in Fig. 13(c). If the foliation is so penetrative that the anisotropy factor is larger than 100, the foliated layer can only deform by simple shear along the direction of the foliation, as long as the major principal stress axis is not perpendicular to the shear zone walls. Figure 13(d) shows how this leads to thinning and transpression of the rock volume involved in the shear motion. Reverse sense of shear would involve thickening and transtension of the shear zone. Foliations oblique to the boundaries of shear zones rotate continuously with respect to the external stress field. Figure 10 illustrates how the mode of progressive deformation will vary as the kinematic vorticity number ranges between 0 and 1 according to the orientation of the principal stress axis with respect to the plane of anisotropy. The magnitudes of the normal and shear strain-rates of the rock between the shear zone boundaries at any time can be calculated by applying the set of equations (18)–(21), and (A1) and (A2). The angle ϕ used in equations (19)–(21) is indicated in Figs. 13(c) & (d).

Folding

Variations in the geometrical details of folds have been extensively described for most of the world's tectonic provinces. The degree and orientation of anisotropy of rocks have figured in previous attempts to explain folding mechanisms (Biot 1961, Cobbold *et al.* 1971). Nonetheless, little attempt has been made to explain how anisotropy may determine the development of various basic types of folds. The distinction between similar and parallel folds on the basis of geometrical features was introduced by Van Hise (1894). *Similar folds* have constant layer thickness if measured parallel to the axial surfaces and *parallel folds* have constant thickness perpendicular to the layer along the fold profile (cf. Ramsay 1967, p. 367). One explanation for the formation of similar folds involves differential simple shear of layers along parallel flow lines (Fig. 14, after Carey 1962). Parallel folds may be formed by tangential longitudinal strain or flexural flow. These three folding mechanisms can be distinguished in the field on the basis of characteristic distribution patterns of refolded lineations (Hobbs *et al.* 1976) or on the basis of strain distribution. It is first explored below how anisotropy may control the occurrence of each of these three folding mechanisms.

(1) *Differential simple shear.* The layers outlining the similar folds of Fig. 14 act merely as passive markers and have no significant mechanical influence. In this approach there is no shortening normal to the streamlines—this is a true shear flow—in contrast to alternative mechanisms discussed by Hudleston (1977, 1983). The problem with Carey's (1962) model for explaining the formation of similar folds is that differential simple shear along the streamlines would require velocity and strain-rate gradients across the fold profile. Such a differential shear is physically impossible in isotropic media but could be explained by the spatial variations in the degree of anisotropy as described in expression (40). Recall Fig. 10 and conclude that a strong anisotropy is simultaneously an efficient mechanism to force simple shear and hinder layer-parallel shortening.

(2) *Simple shear flexure and pure tangential strain.* The two mechanisms currently available to explain the formation of parallel folds (see later) both imply that the initial thickness of the folded layer remains unchanged after folding. This suggests that parallel folds are usually formed in competent layers which do not change length in layer-parallel compression. A question which has remained unanswered in the geoscience literature is: if

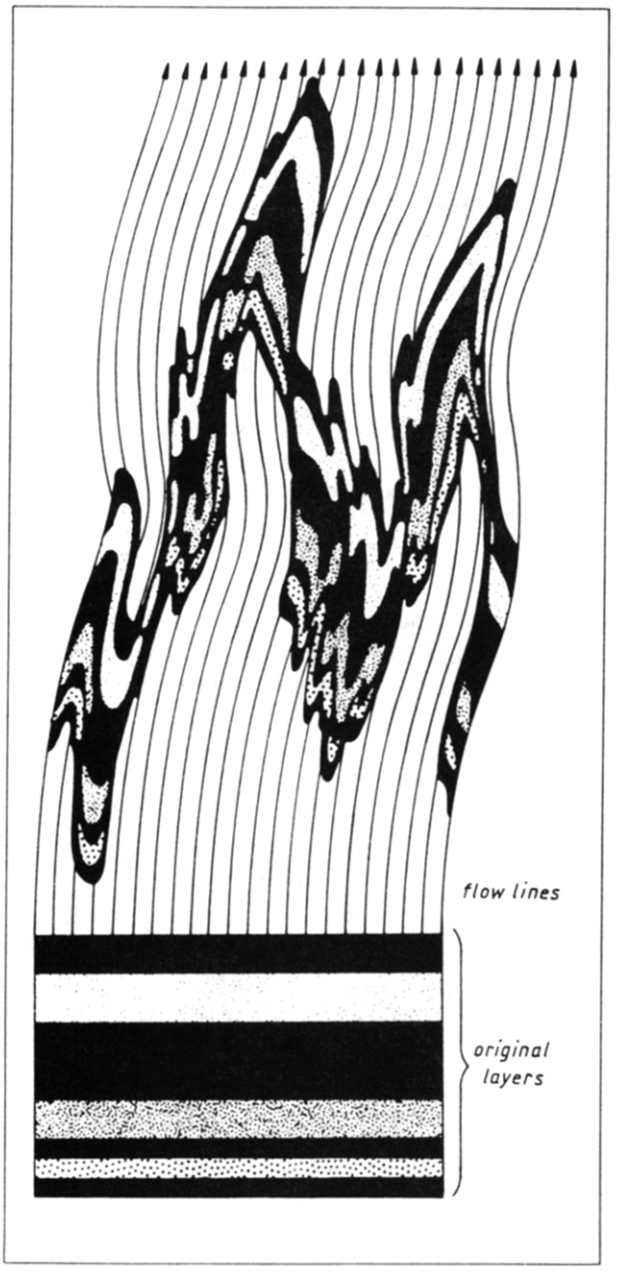

Fig. 14. Ideal similar folds, formed by differential simple-shear flow, involve no shortening normal to the flow lines. Layers act principally as passive markers. The differential simple shear may be explained by spatial variations in the degree of anisotropy parallel to the direction of flow (from Jackson 1985, after Carey 1962).

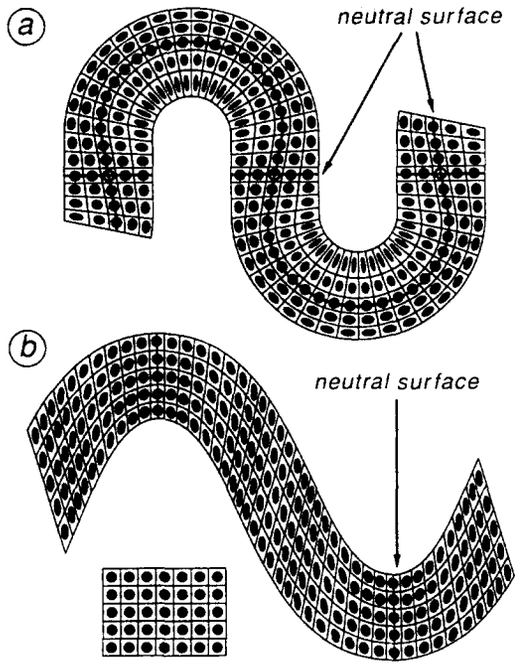

Fig. 15. (a) Parallel fold formed by tangential longitudinal strain (TLS). This type of parallel folding may only occur in competent layers of isotropic viscosity. All strain is due to progressive pure-shear strain with a component of finite rigid-body rotation. Domains of compression and tension are separated by neutral surfaces of zero strain (adapted from Ramsay & Huber 1987, fig. 21.18). (b) Non-concentric parallel folds can only form by flexural shear flow in competent layers if these possess a strong layer-parallel anisotropy. The layer has been shortened to 70% by flexural shear flow, whilst the orthogonal thickness of the layer remains unchanged (adapted from Ramsay & Huber 1987, fig. 21.3).

parallel folds in competent layers can develop by either flexural flow or tangential longitudinal strain, then what determines which mechanism occurs? An explanation is offered below.

Tangential longitudinal strain (Ramsay 1967, p. 398, Ramsay & Huber 1983) confines deformation within the competent layer to progressive pure-shear strain with tangential and radial principal strain trajectories (Fig. 15a). The current distinction between concentric and non-concentric parallel folds was created on a drawing table and has no mechanical implication. In nature strain compatibility rules invariably force natural parallel folds into non-concentric shapes. This is because the difference of finite strains along the inner and outer arcs between two inflection points increases gradually such as to reach maximum values in the axial plane of the fold. This implies that folds formed by tangential longitudinal strain (TLS) can never be truely concentric, and will have non-concentric shapes as illustrated in Fig. 15(a). The neutral surface along the layer is crossed by perpendicular neutral surfaces at the inflection points. This mechanism may operate if the competent layer itself is *isotropic*. Stresses inside the competent layer are then always refracted towards perpendicular orientations with respect to the interface of competency contrast, irrespective of the orientations of the external stress (expression A28).

Another mechanism for forming parallel folds is flexural flow. The deformation pattern produced by flexural flow can be visualized by flexing a stack of computer cards marked with strain circles on the edge (Fig. 15b). This causes a progressive simple-shear deformation with flow along the interfaces of the cards. This simple-shear flow implies that the principal stress axes are consistently oriented at 45° to the surface of flow. Penetrative flexural flow or simple shear along the folded surface therefore implies a strong anisotropy parallel to the layering. More specifically, analytical theory on anisotropic flow predicts that, if the degree of *anisotropy* is sufficiently large (e.g. $\delta > 100$) the principal strain rate axes will always be inclined 45° to the plane of anisotropy, irrespective of the orientation of the principal stress axes (as long as the bulk principal stress axis is not perpendicular to the anisotropy). Conversely, flexural shear flow in a competent layer is unlikely if the internal anisotropy factor δ is much smaller than 100.

Rheology measurements and foliation development

If the anisotropy of rocks is defined by a penetrative foliation (e.g. preferred orientation of grain shape) then the magnitude of the principal viscosities η_N and η_S in the anisotropy factor $\delta = \eta_N/\eta_S$ cannot be obtained analytically. These have to be measured in biaxial laboratory tests with the anisotropy of the samples oriented perpendicular and at 45° to the principal compression direction, respectively. Unfortunately, too few laboratory measurements on the rheology of anisotropic rocks are available, the work of Paterson & Weiss (1966) being a notable exception. Their creep measurements of a fine-grained phyllite suggest an anisotropy factor of $\delta = 2$. Many of the samples, sawn free from the jackets after their creep tests, show the development of kink bands. Expression (40) predicts nucleation of such kink bands by lateral variations in strain rate associated with spatial variations in δ.

One major problem with laboratory creep tests in attempting to determine the rheology of anisotropic materials is that the plane of anisotropy rotates with respect to τ_1 during simple-shear stress measurements (Fig. 16). However, this rotation problem becomes increasingly irrelevant for larger, *retrospectively* determined, anisotropy factors δ. This effect is particularly insignificant for δ larger than, say 100, because the principal strain-rate axes will remain inclined at 45° with respect to the plane of anisotropy, hence maintaining the deformation by effective simple shear only, even if τ_1 is no longer at 45° with respect to the plane of anisotropy. Consequently, this theoretical insight may help to overcome what was addressed by Wenk *et al.* (1986, cf. Paterson 1987) as a serious obstacle to creep tests quantifying the rheology of anisotropic rocks and minerals.

One new implication of the present theory for foliation development arises from the concept that progressive deformation of anisotropic rocks is favourably confined to simple shear in the plane of anisotropy. Any isotropy defined by a grain shape fabric will therefore be *self-enhancing*, because the angle between the long axis

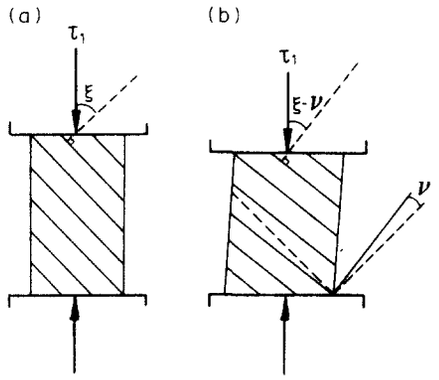

Fig. 16. Section parallel to the compression piston of a creep apparatus and perpendicular to the plane of anisotropy of rock sample. (a) The shear component η_S of the anisotropic viscosity can be determined in such creep apparatus applying a maximum shear stress, so that $\xi = 45°$ at the onset of the experiment. (b) The angle ξ will become progressively smaller during the axial shortening of the rock specimen, but this hardly affects the estimate of η_S if the anisotropy factor $\delta = (\eta_N/\eta_S) > 100$. The normal viscosity component η_N can be measured without any geometric complications by orienting the foliation perpendicular to τ_1 and the piston axis (adapted from Wenk *et al.* 1986, fig. 1).

of any discordant grain and the direction of shear will monotonically decrease during progressive simple shear. If the boundaries of initially equidimensional grains were to act as passive markers, grain shape fabrics will stay perfectly aligned with the finite strain ellipsoid until obliterated by recovery or static recrystallization. The progressive deformation of passive unit spheres by simple shear (isochoric, plane strain) indicates that their major stretching axis S_1 is inclined at 45°, 25°, 20° and 10° with respect to the direction of shear for $S_1 = 1, 2, 3$ and 6, respectively (Fig. 6 and Weijermars 1991). Thin sections of halite polycrystals deformed in bulk simple shear indicate that the crystals indeed tend to align with the orientation of maximum elongation (Shimamoto 1989). Treagus (1983, 1985, 1988) noted that cleavage refracts across the layer interface in isotropic rocks in a fashion similar to that predicted by theory on strain refraction. This view is challenged by experimental observations on a mixture of salt and mica flakes subjected to a bulk pure-shear deformation (Hobbs *et al.* 1982, 1985). In this experiment, the mica flakes were passive markers which could only rotate and fracture, whereas the salt grains deformed by grain boundary migration so that the final grain shape was due to at least two mechanisms. The mismatch between the trace of the strain ellipsoid major axis and the foliation trace was up to 30°. Real-time observations of transparent polycrystals deforming under the microscope also show that grain boundaries are not passive markers (Means 1989), but there is a clear tendency for alignment of the grain shapes with the major bulk strain axis. In other words, once a foliation develops, the degree of anisotropy δ defined by the foliation is likely to increase, until the rate of finite strain accumulation—which decreases with increasing strain—is outpaced by recovery rates. If a balance between strain fabric formation and recovery is reached, the concept of steady-state foliation may be applied (Means 1981) and the anisotropy factor δ will reach a constant value. The extensive literature on cleavage development has been reviewed elsewhere (Siddans 1972, Means 1977, Oertel 1983).

CONCLUSIONS

The possible effect of any anisotropy on the rheological behaviour of rocks has previously been largely neglected, simply because practical analytical methods to describe such flows were not available. An adequate description of anisotropic flow is possible including the normal and shear components of viscosity (η_N and η_S, respectively). The components of the viscosity tensor, in any multilayer comprising individual layers of isotropic viscosity and resolvable thickness, can be calculated on the basis of the intrinsic thickness and viscosity profile alone (equations 19–23). The effective viscosities of the individual layers add up like resistances in series and parallel in the normal and shear viscosities, respectively. Consequently, the resistance to normal compression will be largely determined by the competent layers, whereas the resistance to shear will be controlled by the soft layers.

The degree of anisotropy in any fluid with a rheological structure representable by a normal and shear viscosity can be concisely expressed by the anisotropy factor $\delta = \eta_N/\eta_S$. This ratio of the principal viscosities, initially defined entirely on arbitrary grounds (cf. Honda 1986), appears to have a specific physical meaning. It expresses a measure for the potential misfit in the orientation of the principal axes of the bulk stress and strain-rate ellipsoids (equation 29). For example, the bulk strain-rate ellipsoid will remain consistently inclined at very nearly 45° to the plane of anisotropy, for any orientation of the bulk stress ellipsoid oriented oblique to the layering, provided that the anisotropy factor $\delta > 100$ (Fig. 4). This means that a strongly anisotropic medium may only deform by essentially simple-shear flow constrained within planes normal to the anisotropy, and the direction of flow parallel to the anisotropy.

These results were further tested in an analytical model showing progressive deformation of a unit volume for various anisotropy factors and arbitrary orientations of the principal deviatoric stress. Progressive deformation may be predicted by integrating the rate-of-displacement equations over time and making proper use of the anisotropy factor δ. The results are visualized in a series of nomograms showing the evolution of finite strain and rotation for various degrees of anisotropy (Figs. 6–9). The effect of anisotropy upon the mode of progressive deformation can best be visualized by the relationship between the anisotropy factor, the kinematic vorticity number, and the principal stress orientation (Fig. 10). The derivation of equations governing anisotropic flow provides a basis to explain a variety of ductile deformation processes in nature involving stress and strain refraction (see Appendix).

Practical implications of this theory for anisotropic

flow have been illustrated for progressive deformation in shear zones, folds and foliation development. For example, any shear zone with a strong internal anisotropic fabric parallel to its walls may only deform by simple shear. In contrast, a strong internal anisotropic fabric oblique to the walls implies that the deformation may involve either transpression or transtension, depending upon the orientation of the principal stress axis. The formation of similar folds may be explained by differential simple-shear flow due to spatial variations in the degree of anisotropy. Single competent layers will fold by tangential longitudinal strain if internally isotropic. Such layers will fold by simple-shear flexure if they possess a strong layer-parallel anisotropy. Real folds probably develop by a mechanism intermediate between the two idealizations. Considerations involving the mechanical effects of anisotropic flow lead to the conclusion that grain shape fabrics are self-enhancing until steady-state is reached by the counteractive effect of recovery processes.

Acknowledgements—This paper was critically reviewed and improved from comments by Peter Hudleston and an anonymous reviewer. Jeanette Bergman, Hans Ramberg, Harro Schmeling and Chris Talbot are sincerely thanked for reviewing early versions of this manuscript. I thank Peter Cobbold, Win Means and Susan Treagus for kindly providing offprints of their work on strain refraction in rocks and shear zones. This work has been funded by post-Doctoral research and travel grants of the Swedish Natural Science Research Council (NFR) whilst staying at the Swiss Federal Institute of Technology (ETH) in Zürich (1989).

REFERENCES

Allègre, J. C. & Turcotte, D. L. 1986. Implications of a two-component marble-cake mantle. *Nature* **323**, 123–127.

Backus, G. E. 1962. Long-wave elastic anisotropy produced by horizontal layering. *J. geophys. Res.* **67**, 4427–4440.

Banik, N. C. 1987. An effective anisotropy parameter in transversely isotropic media. *Geophysics* **52**, 1654–1664.

Bayly, M. B. 1970. Viscosity and anisotropy estimates from measurements on chevron folds. *Tectonophysics* **9**, 459–474.

Biot, M. A. 1961. Theory of folding of stratified viscoelastic media and its implications in tectonics and orogenesis. *Bull. geol. Soc. Am.* **72**, 1595–1620.

Biot, M. A. 1965. *Mechanics of Incremental Deformations*. Wiley, New York.

Bobyarchick, A. R. 1986. The eigenvalues of steady flow in Mohr space. *Tectonophysics* **122**, 35–51.

Carey, S. W. 1962. Folding. *Alberta Soc. Petrol. Geol. J.* **10**, 95–144.

Casey, M. & Huggenberger, P. 1985. Numerical modelling of finite-amplitude similar folds developing under general deformation histories. *J. Struct. Geol.* **7**, 103–114.

Christensen, U. 1987. Some geodynamical effects of anisotropic viscosity. *Geophys. J.R.astr. Soc.* **91**, 711–736.

Cobbold, P. R. 1976. Mechanical effects of anisotropy during large finite deformations. *Bull. Soc. géol. Fr.* **18**, 1497–1510.

Cobbold, P. R. 1983. Kinematic and mechanical discontinuity at a coherent interface. *J. Struct. Geol.* **5**, 341–349.

Cobbold, P. R., Cosgrove, J. W. & Summers, J. M. 1971. Development of internal structures in deformed anisotropic rocks. *Tectonophysics* **12**, 23–53.

Cobbold, P. R. & Watkinson, A. J. 1981. Bending anisotropy: a mechanical constraint on the orientation of fold axes in an anisotropic medium. *Tectonophysics* **72**, T1–T10.

Fleitout, A. & Froidevaux, C. 1980. Thermal and mechanical evolution of shear zones. *J. Struct. Geol.* **2**, 159–164.

Flinn, D. 1962. On folding during three-dimensional progressive deformation. *Q. J. geol. Soc. Lond.* **118**, 385–433.

Hobbs, B. E., Means, W. D. & Williams, P. F. 1976. *An Outline of Structural Geology*. Wiley, New York.

Hobbs, B. E., Means, W. D. & Williams, P. F. 1982. The relationship between foliation and strain: an experimental investigation. *J. Struct. Geol.* **4**, 411–428.

Hobbs, B. E., Means, W. D. & Williams, P. F. 1985. The relationship between foliation and strain: an experimental investigation: reply. *J. Struct. Geol.* **7**, 123–124.

Honda, S. 1986. Strong anisotropic flow in a finely layered asthenosphere. *Geophys. Res. Lett.* **13**, 1454–1457.

Hudleston, P. J. 1977. Similar folds, recumbent folds, and gravity tectonics in ice and rocks. *J. Geol.* **85**, 113–122.

Hudleston, P. J. 1983. Strain patterns in an ice cap and implications for strain variations in shear zones. *J. Struct. Geol.* **5**, 455–463.

Jackson, M. P. A. 1985. Natural strain in diapiric and glacial rock salt, with emphasis on Oakwood dome, East Texas. *Bur. Econ. Geol. Rep.* **143**, 1–74.

Jaeger, J. C. & Cook, N. G. W. 1979. *Fundamentals of Rock Mechanics* (3rd edn). Chapman & Hall, London.

Johnson, A. M. 1977. *Styles of Folding*. Elsevier, Amsterdam.

Latham, J.-P. 1985. The influence of nonlinear material properties and resistance to bending on the development of internal structures. *J. Struct. Geol.* **7**, 225–236.

Means, W. D. 1976. *Stress and Strain*. Springer, New York.

Means, W. D. 1977. Experimental contributions to the study of foliations in rocks: a review of research since 1960. *Tectonophysics* **39**, 329–354.

Means, W. D. 1981. The concept of steady-state foliation. *Tectonophysics* **78**, 179–199.

Means, W. D. 1984. Shear zones of types I and II and their significance for reconstruction of rock history. *Am. Soc. Am. Abs. w. Prog.* **16**, 50.

Means, W. D. 1989. Synkinematic microscopy of transparent polycrystals. *J. Struct. Geol.* **11**, 163–174.

Means, W. D. 1990. One-dimensional kinematics of stretching faults. *J. Struct. Geol.* **12**, 267–272.

Means, W. D., Hobbs, B. E., Lister, G. S. & Williams, P. F. 1980. Vorticity and non-coaxiality in progressive deformation. *J. Struct. Geol.* **2**, 371–378.

Nicolas, A. 1989. *Structures of Ophiolites and Dynamics of Oceanic Lithosphere*. Kluwer, Dordrecht.

Nye, J. F. 1957. *Physical Properties of Crystals*. Clarendon Press, Oxford.

Oertel, G. 1983. The relationship of strain and preferred orientation of phyllosilicate grains in rocks—a review. *Tectonophysics* **100**, 413–447.

Paterson, M. S. 1987. Problems in the extrapolation of laboratory rheological data. *Tectonophysics* **133**, 33–43.

Paterson, M. S. & Weiss, L. E. 1966. Experimental deformation and folding in phyllite. *Bull. geol. Soc. Am.* **77**, 343–374.

Pfiffner, O. A. & Ramsay, J. G. 1982. Constraints on geological strain rates: arguments from finite strain states of naturally deformed rocks. *J. geophys. Res.* **87**, 311–321.

Poirier, J.-P. 1980. Shear localization and shear instability in materials in the ductile field. *J. Struct. Geol.* **2**, 135–142.

Ramberg, H. 1975a. Particle paths, displacement and progressive strain applicable to rocks. *Tectonophysics* **28**, 1–37.

Ramberg, H. 1975b. Superposition of homogeneous strain and progressive deformation in rocks. *Bull. geol. Instn. Univ. Uppsala* **6**, 35–67.

Ramberg, H. 1986. Particle paths, displacement and progressive strain applicable to rocks—a correction. *Tectonophysics* **121**, 355.

Ramsay, J. G. 1967. *Folding and Fracturing of Rocks*. McGraw-Hill, New York.

Ramsay, J. G. & Huber, M. I. 1983. *The Techniques of Modern Structural Geology, Volume 1: Strain Analysis*. Academic Press, London.

Ramsay, J. G. & Huber, M. I. 1987. *The Techniques of Modern Structural Geology, Volume 2: Folds and Fractures*. Academic Press, London.

Ribe, N. M. 1989. Seismic anisotropy and mantle flow. *J. geophys. Res.* **94**, 4213–4223.

Ridley, J. & Casey, M. 1989. Numerical modeling of folding in rotational strain histories: Strain regimes expected in thrust belts and shear zones. *Geology* **17**, 875–878.

Saito, M. & Abe, Y. 1984. Consequences of anisotropic viscosity in the earth's mantle (in Japanese with English abstract). *Zisin* **37**, 237–245.

Sanderson, D. J. & Marchini, W. R. D. 1984. Transpression. *J. Struct. Geol.* **6**, 449–458.

Shimamoto, T. 1989. The origin of *S–C* mylonites and a new fault-zone model. *J. Struct. Geol.* **11**, 51–64.
Siddans, A. W. B. 1972. Slaty cleavage, a review of research since 1815. *Earth Sci. Rev.* **8**, 205–232.
Strömgård, K.-E. 1973. Stress distribution during formation of boudinage and pressure shadows. *Tectonophysics* **16**, 215–248.
Simpson, C. 1983. Displacement and strain patterns from naturally occurring shear zone terminations. *J. Struct. Geol.* **5**, 497–506.
Suppe, J. 1985. *Principles of Structural Geology*. Prentice-Hall, Englewood Cliffs, New Jersey.
Treagus, S. H. 1973. Buckling stability of a viscous single-layer system, oblique to the principal compression. *Tectonophysics* **19**, 271–289.
Treagus, S. H. 1981. A theory of stress and strain variations in viscous layers, and its geological implications. *Tectonophysics* **72**, 75–103.
Treagus, S. H. 1983. A theory of finite strain variation through contrasting layers, and its bearing on cleavage refraction. *J. Struct. Geol.* **5**, 351–368.
Treagus, S. H. 1985. The relationship between foliation and strain: an experimental investigation: discussion. *J. Struct. Geol.* **7**, 119–121.
Treagus, S. H. 1988. Strain refraction in layered systems. *J. Struct. Geol.* **10**, 517–527.
Turcotte, D. L. & Schubert, G. 1982. *Applications of Continuum Physics to Geological Problems*. John Wiley, New York.
Van Hise, C. R. 1894. Principles of North American Precambrian geology. *U.S. geol. Surv. Ann. Rep.* **16**, 581–843.
Weijermars, R. 1987a. The Palomares brittle–ductile shear zone of southern Spain. *J. Struct. Geol.* **9**, 139–157.
Weijermars, R. 1987b. The construction of shear strain profiles across brittle–ductile shears. Preliminary estimates of conventional shear strain-rates for the Truchas and Palomares shears (Spain) and the Alpine Fault (New Zealand). *Annales Geophysicae* **5B**, 201–210.
Weijermars, R. 1991. The role of stress in ductile deformation. *J. Struct. Geol.* **13**, 1061–1078.
Weijermars, R. & Rondeel, H. E. 1984. Shear band foliation as an indicator of sense of shear: Field observations in central Spain. *Geology* **12**, 603–606.
Wenk, H. R., Takeshita, T., Van Houtte, P. & Wagner, F. 1986. Plastic anisotropy and texture development in calcite polycrystals. *J. geophys. Res.* **91**, 3861–3869.

APPENDIX

REFRACTION OF STRESS AND STRAIN-RATE AXES AND MAGNITUDE OF STRESS AND STRAIN-RATE IN ANISOTROPIC MULTILAYERS

Expressions are derived below to aid further application of the general equations of flow for orthotropic anisotropy to practical situations. These expressions include simple formulae for calculating the magnitude of the principal stresses (Section A.1) and strain-rates (Section A.2) within all the individual laminae of a multilayer, provided that the external stress field and viscosity are known. The refraction or change in orientation of the principal stress and strain-rate axes across the interface between adjacent layers appears to be an intrinsic property controlled by the viscosity ratio alone (Sections A.3 and A.4). Equations are also derived for determining the angles between the principal axes of bulk strain-rate and bulk stress to the principal axes in individual layers of a multilayer (Section A.5).

A.1. *Magnitude of principal stresses within individual layers of anisotropic multilayers*

The magnitude of the principal stresses, and the normal and shear components of the stress within any individual lamina $a\,(=1,\ldots,q)$ of a multilayer can be analytically calculated. The method applied depends upon whether the multilayer is deformed under a constant bulk stress (case I, τ_1 orientation and magnitude fully known) or a constant bulk strain-rate (case II, $\dot{e}_1$ orientation and magnitude fully known).

(I) First consider the case in which a multilayer is subjected to a constant bulk deviatoric stress τ_1, applied at an arbitrary angle ξ to the normal to the multilayer (Fig. A1). The magnitudes of the bulk normal and shear stresses on the plane of anisotropy are related to the principal deviatoric stresses by the equations for the Mohr circle of stress (cf. Means 1976):

$$\tau_{xx} = \left(\frac{\tau_1 + \tau_3}{2}\right) + \left(\frac{\tau_1 - \tau_3}{2}\right)\cos 2\xi \qquad \text{(A1)}$$

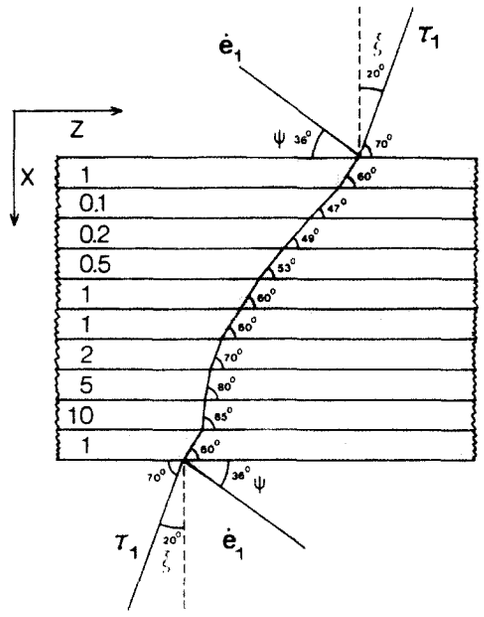

Fig. A1. Illustration of the application of the refraction equations developed in the Appendix. The multilayer comprises 10 beds of equal thickness, so that $d_1^* = d_{10}^* = 0.1$. The magnitude of their normalized effective dynamic viscosities ($\eta_a^* = \eta_a/\eta_o$) is indicated on the layers. The normalized normal and shear viscosities are

$$\eta_N^* = \sum_{a=1}^{10} \eta_a^* d_a^* = 2 \text{ and } \eta_S^* = 1 \Big/ \sum_{a=1}^{10} (d_a^*/\eta_a^*) = 0.5, \text{ respectively.}$$

The anisotropy factor $\delta = 4$. The angles ξ and ψ characterize the orientation of the principal axes of the bulk stress and strain-rate as indicated. The relationship between the bulk angles ξ and ψ is given in expression (29). Bulk angles ξ and ψ are related to angles ξ_a and ψ_a within the multilayer layers by equations (A35)–(A38). Internal refraction is according to expression (A33). Note that there is no difference between ξ_a and ψ_a (for $a = 1$–10) due to the isotropic nature of the effective viscosity within the individual layers of the multilayer. Inspired by fig. 10 of Treagus (1983).

$$\tau_{xz} = \frac{\tau_1 - \tau_3}{2}\sin 2\xi. \qquad \text{(A2)}$$

In incompressible biaxial flow $\tau_1 = -\tau_3$ so that equations (A1) and (A2) yield:

$$\tau_{xx} = \tau_1 \cos 2\xi, \quad \tau_{xx} = -\tau_3 \cos 2\xi \qquad \text{(A3)}$$

$$\tau_{xz} = \tau_1 \sin 2\xi, \quad \tau_{xz} = \tau_3 \sin 2\xi. \qquad \text{(A4)}$$

Consequently, the magnitude of the bulk τ_{xx} and τ_{xz} are known, because they are related to the magnitude of τ_1 by expressions (A3) and (A4).

The magnitude of $\tau_{xx(a)}$ and $\tau_{xz(a)}$ in any of the individual laminae $a(=1,\ldots,q)$ of the multilayer can be calculated from the normal and shear components of the applied bulk stress and the intrinsic material properties η_a and d_a^*:

$$\tau_{xz(a)} = \tau_{xz} \qquad \text{(A5)}$$

$$\tau_{xx(a)} = \tau_{xx}\eta_a/\eta_N = \tau_{xx}\eta_a \Big/ \sum_{a=1}^{q} (\eta_a d_a^*) \qquad \text{(A6)}$$

because $\tau_{xx(a)} = 2\eta_a \dot{e}_{xx(a)} = 2\eta_a \dot{e}_{xx}$, and $\dot{e}_{xx} = \tau_{xx}/2\eta_{xx} = \tau_{xx}/2\eta_N$.

The principal stresses $\tau_{1(a)}$ and $\tau_{3(a)}$ within laminae can then be calculated from the normal and shear stresses $\tau_{xx(a)}$ and $\tau_{xz(a)}$ by the equivalent of equations (A3) and (A4):

$$\tau_{xx(a)} = \tau_{1(a)} \cos 2\xi_a, \quad \tau_{xx(a)} = -\tau_{3(a)} \cos 2\xi_a \qquad \text{(A7)}$$

$$\tau_{xz(a)} = \tau_{1(a)} \sin 2\xi_a, \quad \tau_{xz(a)} = -\tau_{3(a)} \sin 2\xi_a. \qquad \text{(A8)}$$

(II) Secondly, consider a case in which a bulk strain-rate $\dot{e}_1$ is applied

at an arbitrary angle to the multilayer. The magnitude of the bulk $\dot{e}_{xx}$ and $\dot{e}_{xz}$ are also known because they can be calculated from $\dot{e}_1$ and the angle ψ between $\dot{e}_3$ and the plane of anisotropy (Fig. A1):

$$\dot{e}_{xx} = \dot{e}_1 \cos 2\psi, \quad \dot{e}_{xx} = -\dot{e}_3 \cos 2\psi \tag{A9}$$

$$\dot{e}_{xz} = \dot{e}_1 \sin 2\psi, \quad \dot{e}_{xz} = -\dot{e}_3 \sin 2\psi. \tag{A10}$$

The magnitude of $\tau_{xx(a)}$ and $\tau_{xz(a)}$ can now be calculated from the bulk strain-rate components $\dot{e}_{xx}$ and $\dot{e}_{xz}$ by:

$$\tau_{xx(a)} = 2\eta_a \dot{e}_{xx(a)} = 2\eta_a \dot{e}_{xx} \tag{A11}$$

$$\tau_{xz(a)} = \tau_{xz} = 2\dot{e}_{xz}\eta_{xz} = 2\dot{e}_{xz}\eta_S = 2\dot{e}_{xz} \Big/ \sum_{a=1}^{q} (d_a^*/\eta_a). \tag{A12}$$

Subsequently, the principal stresses $\tau_{1(a)}$ and $\tau_{3(a)}$ within the layers $a(=1, \ldots, q)$ can be obtained by applying equations (A7) and (A8).

Note that if $\tau_{xx(a)}$ has been calculated, $\tau_{xx(q)}$ of any other layer can simply be found from the viscosity ratio (cf. equations A6 and A11):

$$\tau_{xx(a)}/\tau_{xx(q)} = \eta_a/\eta_q. \tag{A13}$$

A.2. *Magnitude of principal strain-rates within individual layers of anisotropic multilayers*

Again, consider a multilayer which has its plane of anisotropy perpendicular to the X-axis. All of the deformation is within the XZ-plane and governed by a plane strain-rate ellipsoid with the intermediate axis parallel to the Y-axis so that $\dot{e}_1 = -\dot{e}_3$. The magnitude of the principal strain-rates, and the normal and shear components of the strain-rate in any individual layer a of the multilayer can be analytically obtained. The method depends, again, upon whether the multilayer is deformed under constant bulk stress or constant bulk strain-rate.

(I) If a constant bulk stress is applied, the magnitude of the normal and shear components of principal strain-rate in layer a can be calculated analytically from τ_{xx}, τ_{xz} (obtained from τ_1 by applying expressions A3 and A4), and the intrinsic material properties η_a and d_a^* according to:

$$\dot{e}_{xx(a)} = \dot{e}_{xx} = \tau_{xx}/2\eta_N = \tau_{xx} \Big/ \left(2 \sum_{a=1}^{q} (\eta_a d_a^*)\right) \tag{A14}$$

$$\dot{e}_{xz(a)} = \tau_{xz(a)}/2\eta_a = \tau_{xz}/2\eta_a. \tag{A15}$$

Subsequently, the principal strain-rates $\dot{e}_{1(a)}$ and $\dot{e}_{3(a)}$ within the layers $a(=1, \ldots, q)$ can be obtained from the normal and shear strain-rates $\dot{e}_{xx(a)}$ and $\dot{e}_{xz(a)}$, according to:

$$\dot{e}_{xx(a)} = \dot{e}_{1(a)} \cos 2\psi_a, \quad \dot{e}_{xx(a)} = -\dot{e}_{3(a)} \cos 2\psi_a \tag{A16}$$

$$\dot{e}_{xz(a)} = \dot{e}_{1(a)} \sin 2\psi_a, \quad \dot{e}_{xz(a)} = -\dot{e}_{3(a)} \sin 2\psi_a. \tag{A17}$$

(II) If a constant bulk strain-rate is applied, then $\dot{e}_{xx(a)}$ and $\dot{e}_{xz(a)}$ in layer a can be obtained from $\dot{e}_{xx}$, $\dot{e}_{xz}$ (obtained from $\dot{e}_1$ by applying expressions A9 and A10), and the intrinsic material properties η_a and d_a^* according to:

$$\dot{e}_{xx(a)} = \dot{e}_{xx} \tag{A18}$$

$$\dot{e}_{xz(a)} = \dot{e}_{xz}\eta_S/\eta_a = \dot{e}_{xz} \Big/ \left(\eta_a \sum_{a=1}^{q} (d_a^*/\eta_a)\right) \tag{A19}$$

because $\dot{e}_{xz(a)} = \tau_{xz(a)}/2\eta_a = \tau_{xz}/2\eta_a$ and $\tau_{xz} = 2\eta_{xz}\dot{e}_{xz} = 2\eta_S\dot{e}_{xz}$.

Subsequently the principal strain-rates $\dot{e}_{1(a)}$ and $\dot{e}_{3(a)}$ within the layers $a(=1, \ldots, q)$ can be obtained by applying equations (A16) and (A17). Note that if $\dot{e}_{xz(a)}$ has been solved, $\dot{e}_{xz(q)}$ of any other layer can be found from (cf. equations A15 and A19):

$$\dot{e}_{xz(a)}/\dot{e}_{xz(q)} = \eta_q/\eta_a. \tag{A20}$$

A relationship for the refraction of the incremental strain axes across any rheological interface can be deduced by integrating expressions (A18) and (A19) over time, respectively:

$$e_{xx(a)} = e_{xx(q)} = e_{xx} \tag{A21}$$

$$e_{xz(a)} = e_{xz}\eta_S/\eta_a \tag{A22}$$

or

$$e_{xz(a)} = e_{xz(q)} = \eta_q/\eta_a. \tag{A23}$$

Expression (A23) has been obtained independently by both Cobbold (1983) and Treagus (1983). Current views on the relationship between strain refraction and cleavage development have been discussed by Treagus (1981, 1983, 1988).

A.3. *Inclination angles of principal stress axes within individual layers of anisotropic multilayers*

Imagine a multilayer which has its anisotropy perpendicular to the X-axis. The angle ξ_a between the principal stress axis $\tau_{1(a)}$ and the normal or pole of any layer a (Fig. 4) can be expressed as (from the ratio of equations A7 and A8):

$$\cot 2\xi_a = \tau_{xx(a)}/\tau_{xz(a)}. \tag{A24}$$

For comparison, the relationship between the *total* principal stress and the angle ξ_a is (Turcotte & Schubert 1982, p. 84, equation 2-51):

$$\cot 2\xi_a = (\sigma_{xx(a)} - \sigma_{xz(a)})/2\sigma_{xz(a)}. \tag{A25}$$

Combining expressions (A24) and (A25) and using $\tau_{xz(a)} = \sigma_{xz(a)}$ yields $\tau_1 = (1/2)(\sigma_1 - \sigma_3)$, which is consistent with expressions (2a) and (2c).

Substitution of the expression for the magnitudes of $\tau_{xx(a)}$ and $\tau_{xz(a)}$ obtained in Section A.1 into (A24) gives:

$$\cot 2\xi_a = (\tau_{xx}/\tau_{xz})(\eta_a/\eta_N) \tag{A26}$$

for deformations involving constant bulk stress, and

$$\cot 2\xi_a = (\dot{e}_{xx}/\dot{e}_{xz})(\eta_a/\eta_S) \tag{A27}$$

for deformations due to application of constant bulk strain-rates.

It follows from equations (A26) and (A27), that the angles ξ_a and ξ_q between the plane of anisotropy and the principal stress directions in any pair of layers a and q are related by their viscosity ratio only:

$$\cot 2\xi_a/\cot 2\xi_q = \eta_a/\eta_q. \tag{A28}$$

It is noteworthy that this expression has previously been derived independently by both Strömgård (1973) and Treagus (1973), but without reference to any relationship with the bulk stress axes or the tensor properties of the bulk viscosity.

Note also that:

$$\begin{aligned} \cot 2\xi_a/\cot 2\xi_q &= (\tau_{xx(a)} \cdot \tau_{xz(q)})/(\tau_{xx(q)} \cdot \tau_{xz(a)}) \\ &= (\tau_{xx(a)} \cdot \tau_{xz})/(\tau_{xx(q)} \cdot \tau_{xz}) \\ &= \tau_{xx(a)}/\tau_{xx(q)} \end{aligned} \tag{A29}$$

which independently confirms the validity of expression (A13).

A.4. *Inclination angles of principal strain-rate axes within individual layers of anisotropic multilayers*

Consider a multilayer with its plane of anisotropy oriented consistently perpendicular to the X-axis. The angle ψ_a between the principal strain-rate axis $\dot{e}_{1(a)}$ and the boundary of any layer a (Fig. 4) can be written as (from the ratio of equations A16 and A17):

$$\cot 2\psi_a = \dot{e}_{xx(a)}/\dot{e}_{xz(a)}. \tag{A30}$$

Substitution of the expressions for the magnitudes of $\dot{e}_{xx(a)}$ and $\dot{e}_{xz(a)}$ obtained in Section A.2 yields:

$$\cot 2\psi_a = (\tau_{xx}/\tau_{xz})(\eta_a/\eta_N) \tag{A31}$$

for deformations involving constant bulk stress, and:

$$\cot 2\psi_a = (\dot{e}_{xx}/\dot{e}_{xz})(\eta_a/\eta_N) \tag{A32}$$

for deformations due to application of constant bulk strain-rates.

It follows from equations (A31) and (A32) that the angles ψ_a and ψ_q between the plane of anisotropy and the principal strain-rate directions in any pair of layers a and q is related by their viscosity ratio only:

$$\cot 2\psi_a/\cot 2\psi_q = \eta_a/\eta_q. \tag{A33}$$

Note also that:

$$\begin{aligned} \cot 2\psi_a/\cot 2\psi_q &= (\dot{e}_{xx(a)} \cdot \dot{e}_{xz(q)})/(\dot{e}_{xx(q)} \cdot \dot{e}_{xz(a)}) \\ &= (\dot{e}_{xx} \cdot \dot{e}_{xz(q)})/(\dot{e}_{xx} \cdot \dot{e}_{xz(a)}) \\ &= \dot{e}_{xz(q)}/\dot{e}_{xz(a)} \end{aligned} \tag{A34}$$

which independently confirms the validity of expression (A20).

Figure A2 shows the variation of the angles ξ and ψ across the interface between a competent (subscript c) and incompetent (subscript i) layer with effective viscosity contrast η_c/η_i. Note that large viscosity contrasts (i.e. $\eta_c/\eta_i > 100$) imply that the soft bed will always have angles $\xi_i \approx \psi_i \approx 45°$, irrespective of the orientation of ξ_c and ψ_c in the competent bed, provided that $0° > \xi_c > 90°$.

A.5. *Inclination angles of stress and strain-rate axes in individual laminae related to bulk angles for multilayers*

The angles ξ_a and ψ_a of inclination of the principal stress and strain-rate axes within any individual layer $a(=1, \ldots, q)$, respectively,

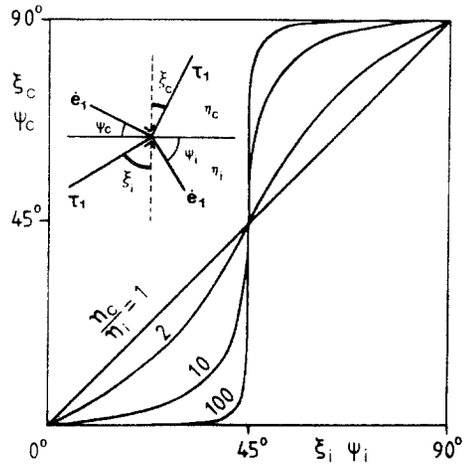

Fig. A2. The refraction of the principal axes of the ellipsoids of stress and strain-rate across an interface separating a competent (c) and incompetent (i) layer quantified in terms of the angles ξ and ψ. Plotted in the diagram are curves for various viscosity contrasts η_c/η_i between the competent and incompetent beds. See also Section A.4 and Fig. A1. (After Treagus 1973, fig. 3.)

are also related to those of the bulk stress and strain-rates (i.e. ξ and ψ) in a very simple fashion. Substitution of expression (25) into (A26) and (A31) gives, respectively:

$$\cot 2\xi_a/\cot 2\xi = \eta_a/\eta_N \tag{A35}$$

$$\cot 2\psi_a/\cot 2\psi = \eta_a/\eta_N. \tag{A36}$$

Substitution of equation (27) into (A27) and (A32) yields, respectively:

$$\cot 2\xi_a/\cot 2\psi = \eta_a/\eta_S \tag{A37}$$

$$\cot 2\psi_a/\cot 2\psi = \eta_a/\eta_S. \tag{A38}$$

Note that the validity of expression (29) can be confirmed independently by dividing either expression (A35) by (A37) or (A36) by (A38). Rule (A28) can also be obtained by using expressions (A35) or (A37), and rule (A33) follows from expression (A36) or (A38).

Combining expressions (A35) and (A38) yields:

$$\cot 2\psi_a/\cot 2\xi_a = (\cot 2\psi/\cot 2\xi)\delta. \tag{A39}$$

The principal axes of stress and strain-rate will be parallel within the individual laminae of isotropic viscosity, so that $\cot 2\psi_a/\cot 2\xi_a = 1$. Insertion of this boundary condition in expression (A39) gives:

$$\tan 2\psi/\tan 2\xi = \delta. \tag{A40}$$

which is similar to expression (29). Reflection on these results reveals that knowledge of only one of the angles ξ_a, ξ, ψ_a, ψ and of the intrinsic material properties δ, η_N, η_S and η_a is sufficient to solve for the other three angles.

CORRIGENDA

Two minor printing errors occurred in expressions (10) and (A8) of the companion paper (Weijermars 1991). In expression (10), the tensor element F_{13} misses the left-hand bracket and should read $(2\dot{e}_{xz}/\dot{e}_{xx})\sinh(\dot{e}_{xx}t)$. In expression (A8), tensor element F_{22} should read 1 and not 0.